arXiv:astro-ph/9901078v1 8 Jan 1999

Electron-Positron Pairs in Hot Accretion Flows and Thin Disk Coronae

Ann A. Esin[1]
Caltech 130-33, Pasadena, CA 91125
aidle@tapir.caltech.edu

ABSTRACT

We investigate equilibrium accretion flows dominated by e^+e^- pairs. We consider one- and two-temperature accretion disk coronae above a thin disk, as well as hot optically thin two-temperature accretion flows without an underlying thin disk; we model the latter in the framework of advection-dominated accretion flows (ADAFs). In all three cases we include equipartition magnetic fields. We confirm the previous result that the equilibrium density of pairs in two-temperature ADAFs is negligible; and show that the inclusion of magnetic fields and the corresponding synchrotron cooling reduces the pair density even further. Similarly, we find that pairs are unimportant in two-temperature coronae. Even when the corona has significantly enhanced heating by direct transfer of viscous dissipation in the thin disk to the corona, the inefficient Coulomb coupling between protons and electrons acts as a bottleneck and prevents the high compactness required for pair-dominated solutions. Only in the case of a one-temperature corona model do we find pair-dominated thermal equilibria. These pair-dominated solutions occur over a limited range of optical depth and temperature.

Subject headings: accretion, accretion disks – black hole physics – plasmas – radiation mechanisms: thermal

1. Introduction

Observational and theoretical efforts to understand the emission from high energy X-ray sources (e.g. AGN and black hole X-ray binaries) have left no doubt about the

[1]AXAF Fellow

existence of astrophysical plasmas with electron temperatures of order $10^9 - 10^{10}\,\mathrm{K}$. As soon as the first hot accretion flow model was constructed (Shapiro, Lightman & Eardley 1976, hereafter SLE) it was realized that the production and annihilation of e^+e^- pairs may play an important role in such solutions. Since then, enormous progress has been made in our understanding of the nature of e^+e^- equilibria, first in the context of static, isothermal hot plasma clouds (e.g. Lightman 1982; Svensson 1982, 1984; Sikora & Zbyszewska 1986; Kusunose 1987; Björnsson & Svensson 1991a), and later for more realistic accretion disk models (e.g. Kusunose & Takahara 1988, 1989, 1990; Tritz & Tsuruta 1989; White & Lightman 1989, 1990; Björnsson & Svensson 1992; Björnsson et al. 1996; Kusunose & Mineshige 1996).

Until now, most treatments of pair equilibria (with the exception of the papers by Zdziarski [1986], Kusunose & Takahara [1989], and Kusunose & Zdziarski [1994]) have considered non-magnetic plasmas, in which the only photon production mechanisms are bremsstrahlung, double Compton scattering and pair annihilation (several authors include also an external soft photon source, e.g. Zdziarski et al. [1994]). However, there exists now a consensus that magnetic fields are universal in accretion flows and play an important role in their energy balance. In the presence of reasonably strong magnetic fields, synchrotron radiation dominates over any other photon production mechanism at mildly relativistic temperatures ($T_e \gtrsim 10^9\,\mathrm{K}$), and the presence of synchrotron photons can change significantly the results obtained for non-magnetized plasmas.

An external source of photons, as in the case of a hot corona above a thin disk (e.g. Haardt & Maraschi 1991, hereafter HM), will also modify the standard e^+e^- pair equilibria. Recently, models for AGN and galactic X-ray binaries based on pair-dominated coronae have been extensively discussed in the literature (e.g. Liang 1991; Zdziarski et al. 1994; Skibo et al. 1995; Stern et al. 1995a, 1995b; Poutanen, Krolik & Ryde 1997). However, to our knowledge, most authors have concentrated on numerical computations of spectra, and have not given enough attention to more basic questions such as the existence and properties of pair equilibria for a range of relevant parameters and assumptions. Kusunose & Mineshige (1991) investigated a two-temperature disk corona, but they explored a relatively narrow parameter range. It is also not clear how their results are related to one-temperature pair-dominated coronae or a popular scenario (suggested originally by HM) in which part of the disk viscous energy is dissipated in the corona. Moreover, since in their model the corona is heated through its own differential rotation, the dynamics of the coronal gas must be treated self-consistently, taking into account the radial energy advection term, especially for the high accretion rates considered in the paper.

In this paper we systematically investigate the existence and properties of pair-

dominated equilibrium solutions for three different scenarios: one-temperature static thin disk coronae, heated by the viscous dissipation of the gravitational energy stored in the disk, two-temperature coronae, and hot accretion flows, similar to those introduced by SLE and Ichimaru (1977, see also Narayan & Yi 1994 and Abramowicz et al. 1995). The latter problem was already discussed by Björnsson et al. (1996) and Kusunose & Mineshige (1996). Our treatment is different only in that we include synchrotron cooling in our calculation, which was left out by the previous authors. The detailed discussion of our initial assumptions and basic equations used for each of the three scenarios are contained in §2. We find that pair-dominated solutions are easy to obtain only in the case of one-temperature coronae, while both two-temperature coronae and hot accretion flows always have negligible pair densities (see §3). These results are discussed in §4. The main conclusions are summarized in §5.

2. Basic Equations

Following Björnsson & Svensson (1991, 1992) we divide the problem of finding equilibrium accretion flow solutions in the presence of e^+e^- pairs into two main parts, one dealing with radiative transfer and pair balance in a static plasma cloud, and the other describing the details of the dynamics and energetics in an accretion flow. Björnsson & Svensson (1991) have shown that the physical properties of a non-magnetized plasma cloud are completely determined by specifying only two parameters. These are the proton optical depth, $\tau_p = n_p \sigma_T H$, and the dimensionless luminosity, or compactness parameter, $\ell = q^- H^2 \sigma_T / m_e c^3$, where H is the size of the cloud, n_p is the proton (i.e. ionized electron) number density, and q^- is the radiative emissivity per unit volume. In this (non-magnetic) case, the mapping between the two parts of the calculation is particularly simple. The accretion flow is treated as a sequence of plasma clouds, whose size is equal to the scale height of the flow. At each point in the flow one needs only to specify ℓ and τ_p in terms of the usual accretion parameters: the mass of the accreting object $m = M/M_\odot$, the radius $r = R/R_S$, where $R_S = 2GM/c^2$, and the accretion rate $\dot{m} = \dot{M}/\dot{M}_{Edd}$, normalized to the Eddington value $\dot{M}_{Edd} = 4\pi G M m_p/(0.1\sigma_T c)$.

In this paper, we attempt to treat a more general problem in which the accretion flow contains strong magnetic fields, which lead to non-negligible cooling via synchrotron radiation. We also allow for external heating and cooling sources which are relevant in a corona heated through dissipation of the thin disk gravitational energy and cooled via Comptonization of thin disk radiation. When these effects are properly taken into account, in addition to the parameters τ_p and ℓ, one needs to specify also the particle density n_p or,

equivalently, the cloud size H, to completely determine the properties of a plasma cloud. With this modification, the mapping between the cloud and flow properties is no longer as straightforward as in Björnsson & Svensson (1991, 1992), and depends on the details of the initial assumptions. Nevertheless, the mapping method is still a convenient technique for solving the problem of electron-positron pairs in accretion flows.

2.1. Pair and Photon Balance in a Hot Plasma Cloud

Pair equilibrium requires that

$$(\dot{n}_+)_{\rm ann} = (\dot{n}_+)_{ee} + (\dot{n}_+)_{ep} + (\dot{n}_+)_{\gamma\gamma} + (\dot{n}_+)_{\gamma e} + (\dot{n}_+)_{\gamma_p}, \tag{2-1}$$

where n_+ is the positron number density, and the rate of pair annihilation on the left hand side is balanced by the sum of pair production rates via $e^\pm$–$e^\pm$, $e^\pm$–p, γ–γ, γ–$e^\pm$, and γ–p collisions, respectively, on the right hand side. We neglect pair escape from the cloud. The analytical expressions for the pair annihilation and electron-electron pair creation rates in a thermal plasma are given by Svensson (1982) and White & Lightman (1989). According to Svensson (1982), the $e^\pm$–p rate can be ignored, since it is generally negligible compared with the $e^\pm$–$e^\pm$ rate. The last three terms in equation (2-1) depend on the photon spectral density and, therefore, involve the details of the radiative transfer which we discuss below.

In a magnetized plasma, thermal synchrotron and bremsstrahlung are the most important photon production mechanisms (in this paper we ignore double Compton scattering). In addition, there might be an external source of soft photons, e.g. blackbody emission from a thin disk irradiating a hot corona. The expressions for thermal bremsstrahlung emissivity are taken from Svensson (1982). The self-absorbed synchrotron emission is modeled using the formalism of Mahadevan et al. (1995) and Narayan & Yi (1995). The magnetic field strength, B, is calculated under the assumption that the gas pressure is in equipartition with the magnetic field pressure in the cloud. For a tangled isotropic magnetic field, this implies that

$$\frac{B^2}{24\pi} = n_p m_e c^2 (\theta_p + (1+2z)\theta_e), \tag{2-2}$$

where $\theta_p = kT_p/m_e c^2$ and $\theta_e = kT_e/m_e c^2$ are dimensionless proton and electron temperatures (both in electron mass energy units), and $z = n_+/n_p$ is the pair fraction. The second term on the right side of equation (2-2) takes into account the pressure from pairs, as well as ionized electrons.

In general, most of the primary photons are too soft to produce pairs. However, when inverse Compton scattering is important, many of the soft photons are boosted up to the

Wien peak. In that case collisions between photons in the Wien peak as well as between Wien and bremsstrahlung photons can dominate pair-production. We follow the approach of Svensson (1984, hereafter S84) and consider the radiation field as a sum of a 'flat' bremsstrahlung continuum and a Wien distribution. In this special case, the photon-particle and photon-photon pair production rate equations can be integrated analytically, and the resulting expressions depend only on the number density of the Wien photons, n_γ.

In order to compute n_γ, we solve the photon balance equation

$$f_B \dot{n}_\gamma^B + f_S \dot{n}_\gamma^S + f_D \dot{n}_\gamma^D = n_\gamma / t_{\rm esc}, \tag{2-3}$$

where $\dot{n}_\gamma^B$, $\dot{n}_\gamma^S$, and $\dot{n}_\gamma^D$ are the rates of bremsstrahlung, synchrotron, and external soft photon production respectively, and f_B, f_S, and f_D represent the fractions of emitted photons that are scattered into the Wien peak before escaping from the cloud. The details of how we compute these quantities are discussed in Appendix A. Finally, we approximate the photon escape time as $t_{\rm esc} = H/c(1+\tau_T g_W(\theta_e))$ (S84), where $\tau_T = (1+2z)\tau_p$ is the total scattering optical depth of the cloud, and the factor $g_W(\theta_e)$ incorporates the Klein-Nishina effect, averaged over the Wien photon distribution.

For fixed θ_e, τ_p and n_p, equations (2-1), (2-2), and (2-3) can be solved to obtain the equilibrium pair fraction $z = n_+/n_p$ and the cloud compactness, ℓ, which in general includes contributions from Comptonized bremsstrahlung and synchrotron emission, as well as Comptonization of the external soft radiation (see Appendix A). As was pointed out by S84, in non-magnetized plasmas the results are practically independent of n_p. The only dependence comes from the determination of the bremsstrahlung self-absorption energy, x_B, defined so that at energies below x_B, the local bremsstrahlung spectrum is a blackbody. The value of x_B is computed using the expression derived by S84. Since the bremsstrahlung energy spectrum is nearly flat, the total emission, as well as the pair production rate, are dominated by the high-energy end of the spectrum, and have at best a logarithmic dependence on x_B, and therefore, n_p. In the presence of magnetic fields, however, the value of the proton number density becomes more important, because it determines the strength of the magnetic field (see equation (2-2)) as well as the value of the synchrotron self-absorption energy, x_S, computed as described in Esin et al. (1996). As opposed to the case of bremsstrahlung radiation, synchrotron emission is generally dominated by the self-absorbed part, so that the dependence on x_S is no longer negligible.

To compare our calculations with previous work, in Fig. 1 we plot the equilibrium pair fraction (panel a) and corresponding compactness (panel b) as functions of the gas temperature $\theta = \theta_e = \theta_p$ for a single-temperature plasma cloud of a fixed size. There is no magnetic field, so that bremsstrahlung is the only source of soft photons. Different curves correspond to different values of τ_p. The results are very similar to those of Svensson

(1982, 1984). For each value of τ_p, there are two equilibrium solutions for temperatures below some critical value, $\theta^c(\tau_p)$; one branch of the solutions (indicated by the solid lines) is pair-dominated, the other (short-dashed lines) is practically pair-free. Above θ^c, the pair production rate is greater than the pair annihilation for any value of z and no equilibrium solution is possible. The critical gas temperature is itself a function of the proton optical depth, increasing with decreasing τ_p, until it reaches a maximum at $\theta^c \sim 24$. The pair-dominated solution branch exists only for $\theta_{BB} < \theta < \theta^c(\tau_p)$, where θ_{BB} is the critical temperature at which the pair fraction reaches its thermal equilibrium value, and the compactness reaches the blackbody limit (the dashed line in Fig. 1(b)).

At low τ_p, the equilibrium values of z on the pair-free solution branch converge to a single curve (Fig. 1(a)), since in this regime, pair production is dominated by particle-particle collisions which have the same scaling with density as the pair annihilation rate (they both vary as τ_p^2). The compactness on the low-z branch is dominated by bremsstrahlung and as a result, varies as τ_p^2 (Fig. 1(b)). The high-z branch, on the other hand, is dominated by photon-photon processes; as a result the pair density is proportional to $1/\tau_p$, while the compactness is independent of the proton optical depth, converging to the Wien equilibrium values for $\theta_e \lesssim 0.4$. The only significant difference between our results and those of S84 is that we overestimate the pair fraction in the temperature range $\theta_e \lesssim 0.1$, where double Compton scattering, which we neglect here, becomes an important source of photons.

Fig. 2 shows how the pair equilibria in a plasma cloud change in the presence of magnetic fields. The magnetic field strength depends on both the electron and proton temperatures (see equation (2-2), and for simplicity the results shown in Fig. 2 were calculated under the assumption that $\theta_p = \theta_e$. A comparison of Figs. 1 and 2 shows that synchrotron cooling significantly changes the shapes of both z and ℓ pair equilibria curves. On the low-z branch, the cloud compactness increases strongly for $\theta_e \gtrsim 0.1$ as compared to the pure bremsstrahlung case. Synchrotron cooling causes the critical temperature to decrease considerably in denser clouds, with $\tau_p \gtrsim 10^{-3}$. By contrast, on the high-z branch the compactness is practically unchanged, since it follows the Wien equilibrium curve. But because of the extra cooling per lepton at temperatures where synchrotron emission is important ($\theta_e \gtrsim 0.1$), the equilibrium pair fraction in a magnetic plasma is up to 10^3 times smaller than in non-magnetic plasmas.

This figure also illustrates the point made previously, that the properties of pair equilibria in magnetized plasmas are *not* independent of the cloud size. For a fixed proton optical depth, a larger cloud has smaller n_p. Therefore, the value of the equipartition magnetic field is smaller as well, reducing the importance of synchrotron cooling. A

comparison between the short-dashed curve computed for a cloud of size $H = 3 \times 10^{14}\,\mathrm{cm}$ and a corresponding curve with the same value of τ_p but $H = 3 \times 10^{7}\,\mathrm{cm}$ shows this effect. It is clear that the dependence on H is not negligible, though it is not very strong. The low-z compactness branch is affected the most, and an increase in H by seven orders of magnitude, causes the value of ℓ to decrease by at most a factor of $\sim 10^{1.5}$.

2.2. Energy Balance

To relate the pair equilibrium solutions calculated for static plasma clouds to a realistic accretion scenario, we must express n_p, τ_p, and ℓ in terms of the accretion parameters $\dot{m}$ and r, and impose an appropriate energy balance condition. Below we describe these mapping relations for two different accretion flow geometries: a corona above a thin disk (§§2.2.1, 2.2.2) and a hot, optically thin accretion flow (§2.2.3).

2.2.1. One-Temperature Disk Coronae

First we consider the simplest scenario, namely a static, hot, one-temperature corona above a cool, geometrically thin, optically thick disk. The study of such coronae was pioneered by HM. The corona is heated through viscous dissipation of the gravitational energy stored in the thin disk (perhaps via magnetic reconnection, e.g. Field & Rogers 1993), and in turn heats the disk by irradiation. Using the formalism of HM, it is easy to show (see Appendix B) that the total emission per unit area from the thin disk, Q_D, is equal to

$$Q_D = Q_G \frac{1 - \delta + \delta\eta(1-a)}{1 - \eta(1-a)(1 - \exp(-\tau_T))}. \tag{2-4}$$

Here $Q_G = 3GM\dot{M}_D/(8\pi R^3)$ is the total viscous dissipation per unit area of the thin disk (e.g. Shakura & Sunyaev 1973; Frank, King, & Raine 1992) with mass accretion rate $\dot{M}_D$, δ is the fraction of viscous energy dissipated directly in the corona, τ_T is the total scattering optical depth in the corona, η is the fraction of radiation emitted or scattered in the corona that is incident on the thin disk, and a is the fraction of incident radiation that is reflected by the disk. In general, η and a depend on the temperature and optical depth of the corona, the ionization state of the thin disk, and the spectrum of irradiating flux. However, since their exact values are not important in light of other approximation made in this work, we adopt the values $\eta = 0.5$ and $a = 0.2$ suggested by HM. This prescription constrains the disk emission to be always in the range $0.4Q_G \le Q_D \le 1.7Q_G$, regardless of the exact values of δ and τ_T. (Note that Q_D is the disk emission as seen by the corona, not by a remote

observer.) We assume that the thin disk radiates as a black body with a color temperature

$$T_D = \left(\frac{Q_D}{\sigma_B}\right)^{1/4}. \tag{2-5}$$

To estimate the characteristic size of the corona, we assume that it is in hydrostatic equilibrium, so that

$$\frac{P}{H} = \rho\frac{GM}{R^2}\ \frac{H}{R} = (m_p n_p + m_e(1+2z)n_p)\frac{GM}{R^2}\ \frac{H}{R}, \tag{2-6}$$

where H is the scale height of the corona, ρ is the mass density, and P includes contributions from the magnetic and gas pressures. It is interesting to note that though in pair-free plasma the contribution of electrons to the mass density in the corona is entirely negligible, if the pair fraction is large enough, namely $z \gtrsim m_p/m_e$, pairs must be properly taken into account. This allows us to solve for the scale height:

$$h = \frac{H}{R} = \sqrt{\frac{2r}{\beta}\ \frac{m_e}{m_p}\ \left[\frac{\theta_p + (1+2z)\theta_e}{1+(1+2z)\frac{m_e}{m_p}}\right]}, \tag{2-7}$$

where $(1-\beta)$ is the ratio of the magnetic field pressure to the total pressure in the corona. In plasmas with no magnetic fields $\beta = 1$. When magnetic fields are taken into account we always assume equipartition between the gas and magnetic field pressure, corresponding to $\beta = 0.5$.

Knowing H, allows us to write the energy balance equation for the corona, by equating compactness ℓ and viscous dissipation (converted into a dimensionless compactness-like quantity):

$$\ell = \frac{\delta Q_G}{H}\ \frac{H^2\sigma_T}{m_e c^3} = \frac{\delta Q_G H \sigma_T}{m_e c^3}. \tag{2-8}$$

To compute the compactness ℓ of the corona, we include contributions from Comptonized bremsstrahlung and synchrotron radiation, as well as inverse Compton scattering of the thin disk photons (see §2.1 and Appendix A for details).

Once the parameters describing the accretion disk (m, r, $\dot{m}_D$) and the corona (δ, τ_p) are fixed, we can solve equations (2-1) through (2-8) to obtain the equilibrium pair fraction and temperature of the corona. We begin by solving pair and photon balance equations for a range of gas temperatures $\theta = \theta_e = \theta_p$. As in the case of a static plasma cloud described in §2.1 above, we obtain two equilibrium curves for $z(\theta)$ and $\ell(\theta)$, slightly modified due to the dependence of the scale height H on θ and z, and the increase in cooling through Comptonization of the thin disk photons. Then we calculate the dimensionless viscous

dissipation rate (the right hand side of equation (2-8)) as a function of temperature, again obtaining two solutions for each value of θ. Finally, we solve for θ such that equation (2-8) is satisfied, i.e. the cooling of the gas in the corona is balanced by viscous dissipation. The results are described in §3.1.

2.2.2. Two-Temperature Coronae

Depending on the microphysical details of how viscosity dissipates gravitational energy, it is feasible that only the protons in the corona are heated directly (e.g. SLE, Rees et al. 1982). Since protons generally cannot radiate, viscous energy must be transfered to the electrons via Coulomb collisions. The Coulomb energy transfer is proportional to the difference between the electron and proton temperatures, so for the gas to be in thermal equilibrium we must have protons hotter than electrons, i.e. $\theta_p > \theta_e$. Such two-temperature plasmas have been often invoked in the literature in the context of hot accretion flows (SLE; Rees et al. 1982; Narayan & Yi 1995; Nakamura, Kusunose, Matsumoto & Kato 1997; Di Matteo, Blackman & Fabian 1997, to give just a few examples) and it is important to investigate how the results for single-temperature coronae are modified when proton-electron energy transfer is explicitly taken into account.

The only difference between one- and two-temperature coronae is that the latter must satisfy two energy balance equations instead of one. Energy balance for the protons requires that viscous heating is equal to the Coulomb energy transfer:

$$q_{ie}H = \delta Q_G. \tag{2-9}$$

For the electrons to be in thermal equilibrium, we must have

$$\ell = \frac{q_{ie}H^2\sigma_T}{m_e c^3}. \tag{2-10}$$

The quantity q_{ie} is the rate of Coulomb energy transfer per unit volume. In our calculations we use the expression for q_{ie} derived by Stepney & Guilbert (1983)

$$\begin{aligned} q_{ie} &= \frac{3}{2}\frac{m_e}{m_p}(1+2z)n_p^2\sigma_T c m_e c^2 \ln\Lambda \frac{(\theta_p-\theta_e)}{K_2(1/\theta_e)K_2(1/\theta_p')} \\ &\quad \times\left[\frac{2(\theta_e+\theta_p')^2+1}{(\theta_e+\theta_P')}K_1\left(\frac{\theta_e+\theta_p'}{\theta_e\theta_p'}\right)+2K_0\left(\frac{\theta_e+\theta_p'}{\theta_e\theta_p'}\right)\right], \end{aligned} \tag{2-11}$$

where K_n is a modified Bessel function of order n, $\theta_p' = \theta_p m_e/m_p$, and the Coulomb logarithm is taken to be $\ln\Lambda = 20$.

To obtain equilibrium solutions for a two-temperature corona, we begin by solving equations (2-1)–(2-7), (2-9), and (2-11) for a range of θ_e, to obtain $z(\theta_e)$, $\ell(\theta_e)$ and $\theta_p(\theta_e)$. Imposing electron energy balance then allows us to determine θ_e, such that equation (2-10) is satisfied. This procedure is very similar to that described in §2.2.1, except that we have an extra energy balance equation, which allows us to solve for θ_e and θ_p separately.

2.2.3. Hot Accretion Flows

In addition to static coronae above a thin disk, we also investigate pair production in pure optically thin, hot accretion flows. Such flows were first proposed by SLE and Ichimaru (1977) and later extensively studied by Narayan & Yi (1994, 1995), Abramowicz et al. (1995), Chen (1995), Chen et al. (1995) and others. Recently, Kusunose & Mineshige (1996) and Björnsson et al. (1996) addressed the problem of pairs in the context of these flows. In this paper we extend their calculations to include the effects of strong thermal synchrotron cooling.

As in two-temperature coronae, the protons in hot accretion flows are heated by viscous dissipation of gravitational energy, which is parameterized in the usual way through the viscosity parameter α. However, we allow for the possibility that only a fraction $(1-f)$ of the dissipated energy is transfered to the electrons via Coulomb collisions. The rest of the energy is stored in the gas as entropy and advected inward with the accretion flow. When the accreting object is a black hole, the stored energy is then lost inside the horizon. With these assumptions, the energy balance equation for the protons takes the form

$$q_{ie}H = (1-f)Q_G, \tag{2-12}$$

where Q_G is the viscous dissipation rate per unit area of the flow, while the energy equation for the electrons is the same as in §2.2.2 above:

$$\ell = \frac{q_{ie}H^2\sigma_T}{m_e c^3}. \tag{2-13}$$

To compute the rate of viscous dissipation, as well as all other relevant quantities in the accreting gas (e.g. n_p, H, equipartition magnetic field strength B, and total pressure P), we use the self-similar solutions derived by Narayan & Yi (1994, 1995). These solutions allow us to express various gas properties as functions of the usual input parameters, m, r, $\dot{m}$, and α as well as the new advection parameter f.

As opposed to the two-zone models discussed above, in hot accretion flows the mass accretion rate $\dot{m}$, which determines the rate of viscous dissipation, and the proton optical

depth τ_p, which specifies the cooling rate of the gas, are not independent parameters. Consequently, to obtain equilibrium accretion flow solutions it is sufficient to specify m, $\dot{m}$, r and α.

We solve for equilibrium solutions in the following manner. For a fixed f, the scale height of the flow and the characteristic sound speed at a given radius r are completely determined by the self-similar solutions. This allows us to solve for the electron temperature θ_e for which the pair balance and electron energy balance equations, (2-1)–(2-3) and (2-13), are satisfied. We then solve for the value of f at which the protons are in thermal equilibrium, determined by equation (2-12).

3. Pair-Dominated Equilibrium Solutions

The aim of this work is to explore whether equilibrium pair-dominated accretion flow solutions exist for different flow geometries and initial assumptions. We present here the results of our calculations for the three models described in §2.2.

3.1. One-Temperature Coronae

Fig. 3 illustrates how equilibrium solutions for a one-temperature corona above a thin disk are determined. On it, we plot the compactness of the corona in pair equilibrium, $\ell(\theta)$, and the corresponding dimensionless viscous dissipation rate as functions of the gas temperature θ. As in the case of a static plasma cloud, both cooling and heating rates have two solutions, which we refer to as the high-z and low-z solutions respectively, for each value of θ. To emphasize the distinction between the high-z and low-z solutions, the former are plotted in Fig. 3 as solid and dashed curves, while the latter are shown by dotted and dot-dashed curves. Energy balance requires that cooling must be balanced by viscous heating; therefore, the point where the two curves intersect, marked by a circle in the figure, is an equilibrium solution for the corona. Because the plot shows two different solution branches simultaneously, it is important to remember that valid solutions correspond only to the intersections of solid lines with dashed lines or dotted lines with dot-dashed lines. The other intersections do not give a solution, since the crossing lines correspond to different values of z.

On panel (a) we show our calculations for proton optical depth $\tau_p = 0.1$, while panel (b) corresponds to $\tau_p = 10^{-5}$. The values of other relevant parameters are given in the figure caption. Note that the relative slopes of the cooling and heating curves are such that

for any choice of $\dot{m}$ and τ_p there is only one intersection point. We do not find multiple solutions for any choice of parameters.

We are interested in pair-dominated solutions, i.e. we wish to find regions of the parameter space in which the high-z branches of cooling and viscous heating have an intersection point. One major trend is clear already from comparing the two panels in Fig. 3; we see that for a fixed mass accretion rate in a thin disk, a corona with a relatively high proton optical depth is pair-free (Fig. 3(a)), while a lower value of τ_p yields a pair-dominated solution (Fig. 3(b)). This trend is easy to understand. The rate of viscous heating is determined by the mass accretion rate in the disk and is relatively independent of τ_p in the corona (if we ignore the slight dependence through the vertical scale height), while the cooling rate on the low-z branch, dominated by Comptonization of the thin disk radiation, decreases linearly with τ_p. Thus, for fixed $\dot{m}_D$, r, and δ, we can find a critical proton optical depth, τ_p^c, below which the corona is pair-dominated, i.e has $z \geq 1$. These maximum values of τ_p for pair-dominated coronae are plotted in Fig. 4(a) as a function of $\dot{m}_D$. The solid line shows our results for a plasma with equipartition magnetic fields. For comparison, we plot τ_p^c for non-magnetized coronae as a dashed line. The two lines are practically identical at high $\dot{m}$, where energy balance in the corona is dominated by Comptonization of disk photons, but begin to diverge at lower $\dot{m}$ where internal cooling in the corona becomes more important.

The other three panels in Fig. 4 illustrate the dependence of τ_p^c on different input parameters. Fig. 4(b) shows how τ_p^c varies as a function of δ, the fraction of the gravitational energy of the gas in the thin disk that is dissipated in the corona. Lower δ means that for the same value of $\dot{m}_D$ the corona is heated less. To compensate for this, we are driven to lower values of τ_p^c to ensure that equation (2-8) is satisfied for $z = 1$. Increasing r, the radial distance from the accretor, has a similar effect on τ_p^c — at larger radii the viscous dissipation rate decreases, which leads to τ_p^c being smaller for a given $\dot{m}_D$ (see Fig. 4(c)). Finally, Fig. 4(d) shows that the results are very similar for low-mass and high-mass accreting black holes. The slight difference between the two curves in due to the fact that the mass of the central object determines the physical scale (H) of the accretion flow (see discussion in section §2.1 and Fig. 2(b)).

In studying pair-dominated corona solutions, two quantities of special interest are the equilibrium temperature and the total optical depth to electron scattering, $\tau_T = (1 + 2z)\tau_p$, since they determine to a large degree the shape of the emitted spectrum. Fig. 5 shows the dependence of these parameters on τ_p for different values of the thin disk mass accretion rate. On every curve, the solution with $z = 1$ (which corresponds to $\tau_p = \tau_p^c$) is marked with a solid dot. To the right of the dot, pairs are not important. Here the scattering

optical depth of the corona is simply equal to τ_p, and the gas temperature increases with decreasing optical depth, to keep up with the cooling. In this regime, our $\theta(\tau_p)$ curve is qualitatively similar to the results of HM, except that for each value of $\dot{m}_D$, there is a maximum allowed τ_p, for which a corona can still be in thermal equilibrium. Above this value, the bremsstrahlung and synchrotron emissivity of the gas in the corona is larger than viscous heating, and thermal equilibrium is not possible.

For $\tau_p < \tau_p^c$, on the other hand, the radiative transfer in the corona is dominated by pairs. In this regime, τ_T initially *increases* with decreasing τ_p, due to copious pair production. Correspondingly, θ decreases, since pairs more than make up for dropping numbers of primary ionized electrons. In the limit $\tau_p \ll \tau_p^c$, the gas in the corona reaches Wien equilibrium, where $z \propto 1/\tau_p$, and as a result, both τ_T and θ converge to constant values, determined solely by $\dot{m}_D$.

A single temperature corona is gravitationally bound when the gas temperature is below the virial value, which we obtain by equating the thermal energy and gravitational energy per proton in the gas:

$$2(1+z)\theta_{vir} = \frac{GM}{Rc^2}\left[\frac{m_p}{m_e} + (1+2z)\right]. \tag{3-1}$$

When $\theta > \theta_{vir}$ the gas in the corona simply escapes from the system on the dynamical time scale. Thus, the solutions calculated here are consistent only for $\theta < \theta_{vir}$. This requirement is equivalent to restricting the scale height of the corona (see equation (2-7)) to $h < 1/\beta$. To check whether this condition is satisfied, we have plotted in Fig. 5(c) $h(\tau_p)$ curves corresponding to equilibrium corona solutions. The thin solid line is drawn for $h = 2$, the stability limit for a corona with equipartition magnetic fields ($\beta = 0.5$). Only those parts of the curves that lie below this line correspond to gravitationally bound solutions. We have seen earlier that the solutions with $z > 1$ exist only to the left of the dots. In other words, pair-dominated and stable coronae exist when $h < 2$ and $\tau_p < \tau_p^c$. These two conditions are mutually exclusive for $\dot{m}_D < 10^{-6}$.

The dot-dashed curves in Fig. 5 show the properties of accretion disk coronae around a supermassive black hole, computed for $mdot_D = 10^{-2}$. As we have seen already, the results are not very sensitive to the black hole mass and there are no qualitative differences between $m = 10$ and $m = 10^8$.

3.2. Two-Temperature Coronae

The gas in a two-temperature corona must satisfy both electron and proton energy balance equations, which require that in thermal equilibrium, compactness, viscous heating and Coulomb energy transfer rate are all equal to one another. First we concentrate on the balance between the two latter quantities, which did not play any role in single-temperature coronae.

The viscous dissipation rate is determined by the mass accretion rate in the thin disk and δ, and is independent of the amount of matter in the corona. The rate of proton cooling via Coulomb collisions, however, varies as a product of the proton and electron+positron densities in the corona, i.e. it is proportional to $(1 + 2z)\tau_p^2$. On the low-z branch, pair density is negligible, so the Coulomb energy transfer rate scales simply as τ_p^2. On the high-z branch, we have $z \propto 1/\tau_p$, so that this quantity is linear in τ_p. In either case, the protons can be in thermal equilibrium only for relatively high values of τ_p. On the other hand, in §3.1 we showed that electron energy conservation in pair-dominated corona solutions requires relatively low values of τ_p. It would appear that the two conditions are mutually exclusive.

Of course in this simplistic argument we have neglected the dependence of both proton cooling and heating rates on particle temperatures and pair density. To get the exact answer we have solved for two-temperature corona solutions numerically, following the procedure described in §2.2.2, exploring the entire $\dot{m}_D - \tau_p$ parameter space. The results are shown on Fig. 6 for two values of δ. Equilibrium solutions are allowed only in the shaded region above the solid ($\delta = 1.0$) or dashed ($\delta = 0.1$) line. A comparison between Figs. 6 and 4(b) clearly shows that these regions lie far above the τ_p^c line, and therefore, must have very few pairs. And indeed, we find that in every case, when an equilibrium corona solution is found, it corresponds to $z < 1$. In other words, we have been unable to find equilibrium pair-dominated two-temperature corona solutions for any choice of parameters.

Our conclusions disagree with those of Kusunose & Mineshige (1991), the only authors, to our knowledge, who investigated e^+e^- pair equilibrium states in a two-temperature corona. This discrepancy stems most likely from different assumptions made in the two studies about the energy source in the corona. In our model, the coronal gas is heated by dissipating the gravitational energy of material in the disk, while Kusunose & Mineshige considered the situation where viscous heating is due to differential rotation of the corona itself. In a sense, their model corresponds to an accretion flow with external soft photon irradiation, rather than a canonical thin disk corona. In fact, the pair equilibrium solutions found by Kusunose & Mineshige (1991) are very similar to those discovered previously by Kusunose & Takahara (1988, 1990) and White & Lightman (1989) in their study of an SLE

accretion disk.

3.3. Hot Accretion Flows

Figs. 7 and 8 demonstrate how we solve for equilibrium solutions in two-temperature hot accretion flows. At a fixed f, $\dot{m}$, and r, the scale height of the accreting gas is fully determined, and therefore, we can compute z, ℓ, and $q_{ie}H^2\sigma_T/(m_e c^2)$ (the dimensionless Coulomb energy transfer rate) as functions of the electron temperature. Compactness and Coulomb energy transfer are plotted in Fig. 7 as solid+dotted and dashed+dot-dashed lines respectively. As usual, we have two branches for each value of θ_e, one with negligible pair density (dotted and dot-dashed lines), and the other dominated by pairs (solid and dashed lines). The transition between the two branches occurs at $z = 0.075$ on panel (a) and at $z = 0.12$ on panel (b). The heating and cooling of the electrons (and pairs) in the flow are balanced only at the intersection points marked in the figure. The two panels show that we can find both high-z and low-z solutions to equation (2-13), depending on the values of f and $\dot{m}$.

It remains now to ensure that the proton energy balance equation (2-12) is satisfied. Since the viscous dissipation rate has the strongest dependence on the advection parameter f, in Fig. 8 we plot it (solid line) as a function of f together with the equilibrium proton cooling rate (dashed lines), obtained by considering electron energy balance as discussed above. The results displayed on panels (a), (b), and (c) differ only by their values of $\dot{m}$, listed in the figure caption.

It is clear from Fig. 8 that there are at most two values of f for which the gas is in thermal equilibrium. The two equilibrium points correspond to the well known solution branches for optically thin accretion flows: the cooling-dominated branch ($f \ll 1$) discovered by SLE, and the advection-dominated branch ($f \sim 1$) proposed by Ichimaru (1977) and rediscovered by Narayan & Yi (1994, 1995) and Abramowicz et al. (1995). Fig. 8(c) shows that at high accretion rates, both solutions disappear. This feature of optically thin accretion flow solutions was pointed out previously by many authors (e.g. Narayan & Yi 1995; Chen et al. 1995).

The question we ask here is whether the properties of the optically thin accretion flow solutions are modified because of the presence of electron-positron pairs. In Fig. 8, the cooling rate corresponding to the low-z compactness branch (see Fig. 7) is indicated by long-dashed lines; short-dashed lines show high-z compactness curves. The actual values of the pair fraction z corresponding to the compactness curves are plotted in Fig. 9. As before,

solid dots mark thermal equilibrium solutions. Note that in every case these equilibria have $z < 1$, implying that pairs do not play an important role in these accretion flows.

To compare these results to previous work on pairs in optically thin accretion flows, it is instructive to plot the thermal equilibrium solutions for optically thin accretion flows at a fixed radius on a $\log \dot{m} - \log \Sigma$ plane. The resulting curves computed for three different values of α are shown in Fig. 10 (thick lines). For comparison, thin lines show equilibrium solutions computed assuming $z = 0$. Consistent with the findings of Kusunose & Mineshige (1996) and Björnsson et al. (1996), the effects of pairs become more pronounced for larger values of α; and are practically negligible for $\alpha < 0.5$. This is mainly because pair production is more efficient in flows with higher density, and therefore, mass accretion rate, and the critical $\dot{m}$ above which thermal equilibrium solutions do not exist, scales roughly as α^2 (Narayan & Yi 1995; Abramowicz et al. 1995). However, even for $\alpha = 1$, pairs contribute no more than $\sim 30\%$ of the total optical depth (see Fig. 10). In fact, we find that the presence of magnetic fields in the flow reduces the importance of pairs even further, as compared with pure bremsstrahlung solutions, since, for a given α, magnetized flows are restricted to lower values of $\dot{m}$ due to extra cooling via synchrotron radiation.

Though the results displayed in Fig. 10 were computed for $m = 10$ we find practically identical results for accretion flows around supermassive black holes.

4. Discussion

From the analysis presented in this paper we conclude that pair-dominated equilibrium solutions exist only in single-temperature disk–plus–corona models. Both two-temperature coronae and single-phase hot accretion flow models have pair fractions $z = n_+/n_p$ significantly below unity. What is the special feature of single-temperature coronae that allows them to be pair-dominated? The answer seems to be that it has fewer constraints then the other two models.

The gas in the corona is heated via viscous dissipation of energy in an underlying thin disk. The rate of such heating is completely determined by the properties of the thin disk (namely, mass accretion rate $\dot{m}_D$ and radius r) and is virtually independent of the amount or temperature of matter in the corona, which specify the cooling rate. Thus, for a given value of $\dot{m}_D$, the energy balance in the corona allows us to solve for either τ_p or θ, but not both. One of these parameters has to be specified as an initial condition. This extra degree of freedom allows us to adjust the mass accretion rate in the disk and the optical depth of the corona to obtain thermal equilibrium solutions with $z > 1$. We find that such solutions

are restricted to $\tau_p < \tau_p^c$, where the critical value of the proton optical depth decreases with decreasing $\dot{m}_D$ (see Fig. 4).

In a two-temperature corona, heating and cooling rates are still relatively independent of each other; however, proton energy balance imposes an important additional constraint on the model. The proton cooling rate via Coulomb scattering between protons and electrons (as well as pairs) is sensitive to the number density of particles in the corona, while proton heating through viscous dissipation is independent of τ_p. Consequently, protons are in thermal balance only for relatively high values of τ_p. But at these values of τ_p, electron energy balance requires $z < 1$ (Fig. 6).

In the single-phase hot accretion flow model, both viscous heating and radiative cooling rates are determined by the mass accretion rate in the flow. In this model, $\dot{m}$ specifies both the optical depth and temperature of the accreting gas; one can no longer adjust these variables independently in order to obtain pair-dominated solutions. We find that for a realistic range of values for the viscosity parameter α, the pair density in hot accretion flows is negligible, both for the cooling-dominated (SLE) and the advection-dominated (Ichimaru 1977, Narayan & Yi 1994) solution branches. In the two-temperature accretion flow solution we have considered, the Coulomb energy transfer bottleneck also plays a role in limiting the effects of pairs.

Even in one-temperature coronae, we find that pair-dominated solutions exist only over a relatively narrow range of the proton optical depth, for each value of $\dot{m}_D$ (see Fig. 5(c)). It is bounded from above by τ_p^c, imposed by the thermal equilibrium balance equation for the gas, and from below by the requirement that the hot gas in the corona should be gravitationally bound. The latter condition can be somewhat relaxed, if we assume that the corona is held in place not by gravity, but rather by magnetic field loops anchored in the thin disk. In fact, the most popular recent scenario for the dissipation of the thin disk gravitational energy in the corona is based on reconnection of the magnetic field loops generated in the disk and transported by buoyancy into the corona (Galeev, Rosner & Vaiana 1979; Field & Rogers 1993). In this picture, if the magnetic energy density dominates the energy density of the gas, magnetic fields may prevent the escape of particles from the corona even if their temperature is above virial. On the other hand, if the cooling of the gas in the corona is dominated by inverse Compton scattering of the thin disk photons, electrons and positrons can undergo a considerable radiative acceleration along the accretion disk poles (see for example Liang & Li [1995], Li & Liang [1996]), which may allow the escape of pairs with temperatures below virial.

When we consider a one-temperature accretion disk corona with $\theta_e = \theta_p$, an important question to ask is what keeps electrons and protons at the same temperature. If viscous

dissipation preferentially heats the protons, as is often assumed in the literature (e.g. SLE; Rees et al. 1982; Narayan & Yi 1995), the electrons will be considerably cooler than the heavier particles. Our results for two-temperature coronae clearly show that Coulomb energy transfer is too inefficient to equilibrate θ_e and θ_p. One way to solve this problem is to introduce some other more efficient energy transfer mechanism between the protons and electrons in the corona (e.g. Begelman & Chiueh 1988). On the other hand, recent work on dissipation mechanisms for MHD waves by Quataert (1998) and Gruzinov (1998) indicate that in magnetically dominated plasma it is electrons, rather than the protons that are preferentially heated. In this case, the protons might even be cooler than the electrons (if the accretion timescale is shorter than the Coulomb energy transfer timescale). However, since it is the latter that contribute to cooling and pair-production, θ_p is practically irrelevant, so that the corona can be treated as a single-temperature gas cloud.

Finally, we would like to emphasize that the results for thin disk coronae presented in this paper apply only to steady-state, homogeneous corona scenarios such as discussed, for example, by Haardt & Maraschi (1991, 1993), as opposed to time-dependent flare models in which a corona contains many localized active regions (e.g. Haardt, Maraschi & Ghisellini 1994; Stern et al. 1995b, Nayakshin & Melia 1997a,b; Di Matteo, Celotti & Fabian 1997, 1998). In the latter case, many of the constraints imposed to find the equilibrium solutions need not be satisfied. In particular, the protons may transfer only part of the viscously dissipated energy to the electrons and pairs. In that case, the protons will experience a net heating, until they reach virial temperature and escape from the system, perhaps in the form of an outflow or a jet. After that more material will be evaporated into the corona from the disk, and the cycle will be repeated. Similarly, the pairs themselves may be periodically ejected from the corona driven either by radiative acceleration (Liang & Li 1995) or simply through heating above their virial temperature, in the absence of energy balance. Such transient or time-dependent situations are beyond the scope of the paper.

5. Summary

We find that the properties of pair equilibria in static plasma clouds, taking into account synchrotron emission and Comptonization of external soft photons differ only in quantitative details from the results of S84, who restricted his study to Comptonized bremsstrahlung and double Compton emission. For every value of the proton optical depth, τ_p, there exists a critical electron temperature $\theta_{max}(\tau_p)$ below which there are two pair equilibrium solution branches, one of which is pair-dominated, and the other practically pair-free. On the pair-free branch, particle-particle pair production processes dominate

and the pair fraction $z = n_+/n_p$ is independent of τ_p. By contrast, on the pair-dominated branch the electron (and positron) scattering optical depth is constant, so that $z \propto 1/\tau_p$. The extra sources of photons considered here (synchrotron and external photons) do not change the general character of the solutions, but they do decrease the value of θ_{max} so that pair equilibria are restricted to lower temperatures than in S84.

We studied in this paper three popular accretion scenarios involving hot plasmas to assess the importance of pairs. Our results for the three models are summarized below:

1) In the case of a single-temperature corona above a thin disk, the cooling of the gas must be balanced by viscous heating. The latter quantity is determined by the mass accretion rate, $\dot{M}_D$, in the thin disk and the fraction δ of the viscous energy which is dissipated in the corona. The compactness on the low-z branch is due primarily to inverse Compton scattering of synchrotron and thin disk photons, so that $\ell \propto \tau_p$. As a result, for every value of the mass accretion rate in the thin disk, we find that there is a critical τ_p^c in the corona below which the equilibrium solution is pair-dominated (see Fig. 4). For larger values of τ_p, pairs in the corona are unimportant. Thus, while pure pair coronae are allowed, such coronae have very little mass and are dominated by energy deposition from the disk.

2) A two-temperature corona above a thin disk must satisfy two energy conservation equations, one for electrons and one for protons. That is, the Coulomb energy transfer rate must balance both the rate of viscous energy input into the protons and the the cooling rate of the electrons. Since the Coulomb energy transfer is a two-body process, it is proportional to τ_p^2 on the low-z pair equilibrium branch and goes as $z\tau_p^2 \propto \tau_p$ on the high-z branch. We find that the extra constraint on the energy balance (compared to a single-temperature corona) restricts solutions to relatively high values of the proton optical depth. Only at such τ_p is Coulomb coupling efficient enough. However, the critical τ_p is generally above the maximum τ_p^c up to which pair-dominated coronae are possible (see Figs. 4 and 6). Thus, we conclude that, if viscous dissipation heats primarily the protons in the corona, the equilibrium solutions are generally pair-free.

3) Finally, we have considered pair equilibria in hot accretion flows described by the self-similar solution of Narayan & Yi (1995). We find that the energy transfer bottleneck due to Coulomb coupling conspires with the advective cooling in these flows to limit the effects of e^+e^- pairs. We agree with the results of earlier investigators (Björnsson et al. 1996 and Kusunose & Mineshige 1996) who concluded that for reasonable values of the viscosity parameter ($\alpha \lesssim 0.5$) there are no pair-dominated solutions on either the advection-dominated or cooling-dominated (i.e. SLE) branches.

Previous work dealt only with Comptonized bremsstrahlung cooling. We have included Comptonized synchrotron here, but recover the same results as before with only minor quantitative differences (Fig. 10).

I would like to thank Ramesh Narayan for numerous useful discussions and suggestions. This work was supported in part by National Science Foundation Graduate Research Fellowship, and by NASA through AXAF Fellowship grant #PF8-10002 awarded by the AXAF Science Center, which is operated by the Smithsonian Asprophysical Observatory for NASA under contract NAS8-39073.

A. Inverse Compton Scattering

A.1. Analytical Formalism

We treat inverse Compton scattering of photons by thermal electrons using the approximate analytical formulae derived by S84 and Esin et al. (1996).

When the plasma cloud is optically thin, $\tau_T < 1$, the probability $\mathcal{P}_j$ that a photon will suffer exactly j scatterings before escaping can be approximated by a Poisson formula:

$$\mathcal{P}_j = \frac{e^{-s} s^j}{j!}, \tag{A1}$$

where $s = \tau_T + \tau_T^2$ is the mean number of scatterings (Rybicki & Lightman 1979). If the initial photon energy, $x = h\nu/m_e c^2$ is small compared with the thermal energy of the electrons in the cloud, on average, each scattering will increase the photon energy by a factor $A = 1 + 4\theta_e + 16\theta_e^2$ (Rybicki & Lightman 1979). This process saturates when the photon energy becomes comparable to the average energy of the Wien distribution, $3\theta_e$. Thus, the number of scatterings corresponding to saturation is $j_m = \ln(3\theta_e/x)/\ln A$. Then the fraction of photons with initial energy x that are scattered into the Wien peak before escaping is simply

$$f(x) = \sum_{j=j_m}^{\infty} \mathcal{P}_j = \frac{3\theta_e}{x} P(j_m, s), \tag{A2}$$

where $P(j_m, s) = \int_0^s e^{-y} y^{j_m - 1} dy/\Gamma(j_m)$, is the incomplete gamma function (see Esin et al. [1996] for a detailed derivation of this formula).

The energy gain through Comptonization is characterized by the average energy enhancement factor for each photon, ξ, defined as the ratio of the photon final and initial energies:

$$\xi(x) = \sum_{j=0}^{j_m} A^j \mathcal{P}_j + A^{j_m} \sum_{j=j_m+1}^{\infty} \mathcal{P}_j = e^{(A-1)s}[1 - P(j_m + 1, As)] + \frac{3\theta_e}{x} P(j_m + 1, s). \tag{A3}$$

For an optically thick cloud, $\tau_T > 1$, we use a different expression for probability $\mathcal{P}_j$, derived by Sunyaev & Titarchuk (1980, see also S84),

$$\mathcal{P}_j = \frac{e^{-j/(3\tau_T^2)}}{3\tau_T^2}. \tag{A4}$$

Since in this regime each photon will undergo many scatterings before escaping, we can treat j as a continuous variable (the expression for $\mathcal{P}_j$ is normalized accordingly). Then the

fraction of photons scattered into the Wien peak can be written as an integral:

$$f(x) = \int_{j=j_m}^{\infty} \mathcal{P}_j = \exp\left[-\frac{\ln(3\theta_e/x)}{3\tau_T^2 \ln A}\right]. \tag{A5}$$

Note that this expression differs slightly from that derived by S84 (equation C3), since we assume that the average energy of Wien photons is $3\theta_e$, rather than θ_e.

The average energy enhancement factor for photons is then

$$\xi(x) = \int_0^{j_m} A^j \mathcal{P}_j + A^{j_m} \int_{j_m}^{\infty} \mathcal{P}_j = \left[\frac{(3\theta_e/x)f(x) - 1}{3\tau_T^2 \ln A - 1}\right] + \frac{3\theta_e}{x} f(x). \tag{A6}$$

In our calculations we simply use equations (A2) and (A3) when $\tau_T < 1$ and equations (A5) and (A6) when $\tau_T > 1$, with a suitable interpolation across $\tau_T = 1$.

A.2. Comptonization of Bremsstrahlung Photons

Bremsstrahlung photon emissivity is given by a normalized expression (S84)

$$S_B dx = 2\frac{\ln(\theta_e/x)}{\ln^2(\theta_e/x_B)}\frac{dx}{x}, \qquad x_m < x < \theta_e, \tag{A7}$$

where x_B is the bremsstrahlung self-absorption energy, computed by comparing the bremsstrahlung and Compton scattering absorption coefficients (for details see appendix D of S84). Then the emission weighted fraction f_B is simply

$$f_B = \int_{x_B}^{\theta} f(x) S_B(x) dx, \tag{A8}$$

while the total energy amplification factor for bremsstrahlung emission is

$$\xi_B = \frac{\int_{x_B}^{\theta} x\xi(x) S_B(x) dx}{\int_{x_B}^{\theta} x S_B(x) dx}, \tag{A9}$$

In the optically thick limit, equations (A8) and (A9) can be evaluated analytically (S84):

$$f_B = 2\exp\left(-\frac{\ln 3}{3\tau_T^2 \ln A}\right)[y^2 - (y + y^2)e^{-1/y}], \tag{A10}$$

and

$$\xi_B = 1 + f_B \frac{3}{4} \ln^2\left(\frac{\theta_e}{x_B}\right). \tag{A11}$$

where $y = 3\tau_T^2 \ln A / \ln(\theta_e / x_B)$ is the emission averaged Compton y-parameter.

In the optically thin regime, we integrate equations (A8) and (A9) numerically.

The rate of Wien photon production due to Compton upscattering of bremsstrahlung photons is simply $f_B \dot{n}_\gamma^B$. We use the expression for n_γ^B, volume emissivity of bremsstrahlung photons via $e^\pm e^\pm$ and $e^\pm p$ interactions, derived by S84 (equations A1-A3 and A22a). Total Comptonized bremsstrahlung cooling rate per unit volume is $\xi_B q_B$, where q_B is the thermal bremsstrahlung cooling rate per unit volume (Svensson 1982).

A.3. Comptonization of Synchrotron Photons

Thermal synchrotron emission is generally strongly self-absorbed, so that most of the emission comes out near the self-absorption frequency x_S, calculated as described in Esin et al. (1996). When calculating the effect of Comptonization, this means we can treat synchrotron emission as a monochromatic source of photons, characterized by a photon production rate $\dot{n}_\gamma^S = q_S/(x_S m_e c^2)$. Here q_S is the synchrotron cooling rate per unit volume, for which we employ the expressions derived by Mahadevan et al. (1995) and Esin et al. (1996). Then the rate of Wien photon production due to upscattering of synchrotron photons is $f_S \dot{n}_\gamma^S = f(x_S)\dot{n}_\gamma^S$. Similarly, total Comptonized synchrotron cooling rate is just $\xi_S q_S = \xi(x_S) q_S$.

A.4. Comptonization of Thin Disk Photons

Since thin disk emission has a thermal spectrum, we can treat it in exactly the same way as the synchrotron emission – as a monochromatic source of photons with energy $x_D = 2.8kT_D/m_e c^2$. The characteristic temperature T_D is given by equation (2-5). Then the rate of production of the thin disk photons per unit volume of the corona is $\dot{n}_\gamma^D = Q_D/(H x_D m_e c^2)$, where cooling rate per unit area of the disk, Q_D, is given by equation (2-4). Consequently, we can write the rate of upscattering of disk photons into the Wien peak as $f_D \dot{n}_\gamma^D = f(x_D)\dot{n}_\gamma^D$.

The cooling rate of gas in the corona through inverse Compton scattering of thin disk photons is then $(\xi_D - 1)Q_D/H = (\xi(x_D) - 1)Q_D/H$.

B. Emission from the Thin Disk

Following HM we approximate disk and corona as two uniform adjacent slabs, characterized by different temperatures and densities. The rate of gravitational energy release per unit area is Q_G, of which a fraction δ is dissipated directly in the corona, while the remaining $(1-\delta)Q_G$ is dissipated within the thin disk.

The cold optically thick disk radiates as a blackbody, with a total flux Q_D. On the other hand, the optically thin corona cools by emitting Comptonized synchrotron and bremsstrahlung radiation, as well as through inverse Compton scattering of the thin disk photons. Total cooling rate per unit ares of the corona can be written as $Q_C = Q_{SB} + (\xi - 1)Q_D$, where the first term stands for the internal coronal emission and ξ is amplification factor due to Comptonization of the thin disk emission. The energy balance for the corona requires that

$$\delta Q_G = Q_{SB} + (\xi - 1)Q_D. \tag{B1}$$

We assume further that a fraction η of all photons emitted of scattered in the corona is directed downwards towards the thin disk, while the remaining radiation escapes towards the observer. Then the total flux incident onto the thin disk can be written as

$$Q_{inc} = \eta[Q_{SB} + (\xi - 1)Q_D + Q_D(1 - \exp(-\tau_T))], \tag{B2}$$

where τ_T is the optical depth of the corona to electron scattering, and $(1 - \exp(-\tau_T))$ is the fraction of the thin disk photons scattered at least once before escaping. This incident radiation is partly absorbed by the thin disk, heating it further, and partly reflected. We write the absorbed fraction as $(1-a)Q_{inc}$.

Note that equation (B2) above differs from the corresponding expression in HM in two ways. Firstly, we include the internal emission from the corona. Secondly, we take into account the fact that the corona not only amplifies thin disk emission through Compton scattering, it also acts as a reflector for the thin disk photons. In the limit when Comptonization is not important, i.e. $\xi \simeq 1$, the presence of the corona still raises the equilibrium temperature of the disk through the greenhouse effect.

With this, we can write down the energy balance equation for the disk:

$$(1 - \delta Q_G) + (1-a)\eta[Q_{SB} + (\xi - 1)Q_D + Q_D(1 - \exp(-\tau_T))] = Q_D. \tag{B3}$$

Combining equations (B1) and (B3), we obtain the expression for total disk emission, which is independent of the details of inverse Compton scattering in the corona:

$$Q_D = Q_G \frac{1 - \delta + \delta\eta(1-a)}{1 - \eta(1-a)(1 - \exp(-\tau_T))}. \tag{B4}$$

REFERENCES

Abramowicz, M. A., Chen, X., Kato, S., Lasota, J. P., & Regev, O. 1995, ApJ, 438, L37

Begelman, M. C. & Chiueh, T. 1988,ApJ, 332, 872

Björnsson, G., Abramowicz, M. A., Chen, X., & Lasota, J.-P. 1996, ApJ, 467, 99

Björnsson, G. & Svensson, R. 1991a, MNRAS, 249, 177

Björnsson, G. & Svensson, R. 1991b, ApJ, 371, L69

Björnsson, G. & Svensson, R. 1992, ApJ, 394, 500

Chen, X. 1995, MNRAS, 275, 641

Chen, X., Abramowicz, M. A., Lasota, J. P., Narayan, R., Yi, I. 1995, ApJ, 443, L61

Di Matteo, T., Blackman, E. G., & Fabian, A. C. 1997, MNRAS, 291, L23

Di Matteo, T., Celotti, A., Fabian, A. C. 1997, MNRAS, 291, 805

Di Matteo, T., Celotti, A., Fabian, A. C. 1998, astro-ph/9805345

Esin, A. A., Narayan, R., Ostriker, E., & Yi, I. 1996, ApJ, 465, 312

Field, G. B., & Rogers, R. D. 1993, ApJ, 403, 94

Frank, J., King, A., & Raine, D. 1992, Accretion Power in Astrophysics (Cambridge, UK: Cambridge University press)

Galeev, A. A., Rosner, R. & Vaiana, G. S. 1979, ApJ, 229, 318

Gruzinov, A. V. 1998, ApJ, in press

Haardt, F. & Maraschi, L. 1991, ApJ, 380, 51 (HM)

Haardt, F. & Maraschi, L. 1993, ApJ, 413, 507

Haardt, F., Maraschi, L. & Ghisellini, G. 1994, 432, L92

Nayakshin, S. & Melia, F. 1997a, ApJ, 490, L13

Nayakshin, S. & Melia, F. 1997b, submitted to ApJL, astro-ph/9709286

Ichimaru, S. 1977, ApJ, 214, 840

Li, H. & Liang, E. P. 1996, ApJ, 458, 514

Liang, E. P. 1991, ApJ, 367, 470

Liang, E. P. & Li, H. 1995, A&A, 298, L45

Lightman, A. P. 1982, ApJ, 253, 842

Kusunose, M. 1987, ApJ, 321, 186

Kusunose, M. & Mineshige, S. 1996, ApJ, 468, 330

Kusunose, M. & Mineshige, S. 1991, ApJ, 381, 490

Kusunose, M. & Takahara, F. 1988, PASJ, 40, 435

Kusunose, M. & Takahara, F. 1989, PASJ, 41, 263

Kusunose, M. & Takahara, F. 1990, PASJ, 42, 347

Kusunose, M. & Zdziarski, A. A. 1994, ApJ, 422, 737

Mahadevan, R., Narayan, R., Yi, I. 1996, ApJ, 465, 327

Nakamura, K. E., Kusunose, M., Matsumoto, R., Kato, S. 1997, PASJ, 49, 503

Narayan, R. & Yi, I. 1994, ApJ, 428, L13

Narayan, R. & Yi, I. 1995, ApJ, 452, 710

Poutanen, J., Krolik, J. H., & Ryde F. 1997, MNRAS, 292, L21

Quataert, E. 1998, ApJ, in press

Rees, M. J., Begelman, M. C., Blandford, R. D., Phinney, E. S. 1982, Nature, 295, 17

Rybicki, G. B. & Lightman, A. P. 1979, Radiative Processes in Astrophysics (New York: John Wiley & Sons)

Shakura, N. I. & Sunyaev, R. A. 1973, A&A, 24, 337

Shapiro, S. L., Lightman, A. P., & Eardley, D. M. 1976, ApJ, 204, 187 (SLE)

Sikora, M. & Zbyszewska, M. 1986, Acta Astron., 36, 255

Skibo, J. G., Dermer, C. D., Ramaty, R., McKinley, J. M. 1995, ApJ, 446, 86

Stepney, S. & Guilbert, P. W. 1983, MNRAS, 204, 1269

Stern, B. E., Begelman, M. C., Sikora, M., & Svensson, R. 1995a, MNRAS, 272, 291

Stern, B. E., Poutanen, J., Svensson, R., Sikora, M., Begelman, M. C. 1995b, ApJ, 449, L13

Svensson, R. 1982, ApJ, 258, 335

Svensson, R. 1984, MNRAS, 209, 175 (S84)

Tritz, B. G. & Tsuruta, S. 1989, ApJ, 340, 203

White, T. R. & Lightman, A. P. 1989, ApJ, 340, 1024

White, T. R. & Lightman, A. P. 1990, ApJ, 352, 495

Zdziarski, A. A. 1986, ApJ, 303, 94

Zdziarski, A. A. et al. 1994, MNRAS, 269, L55

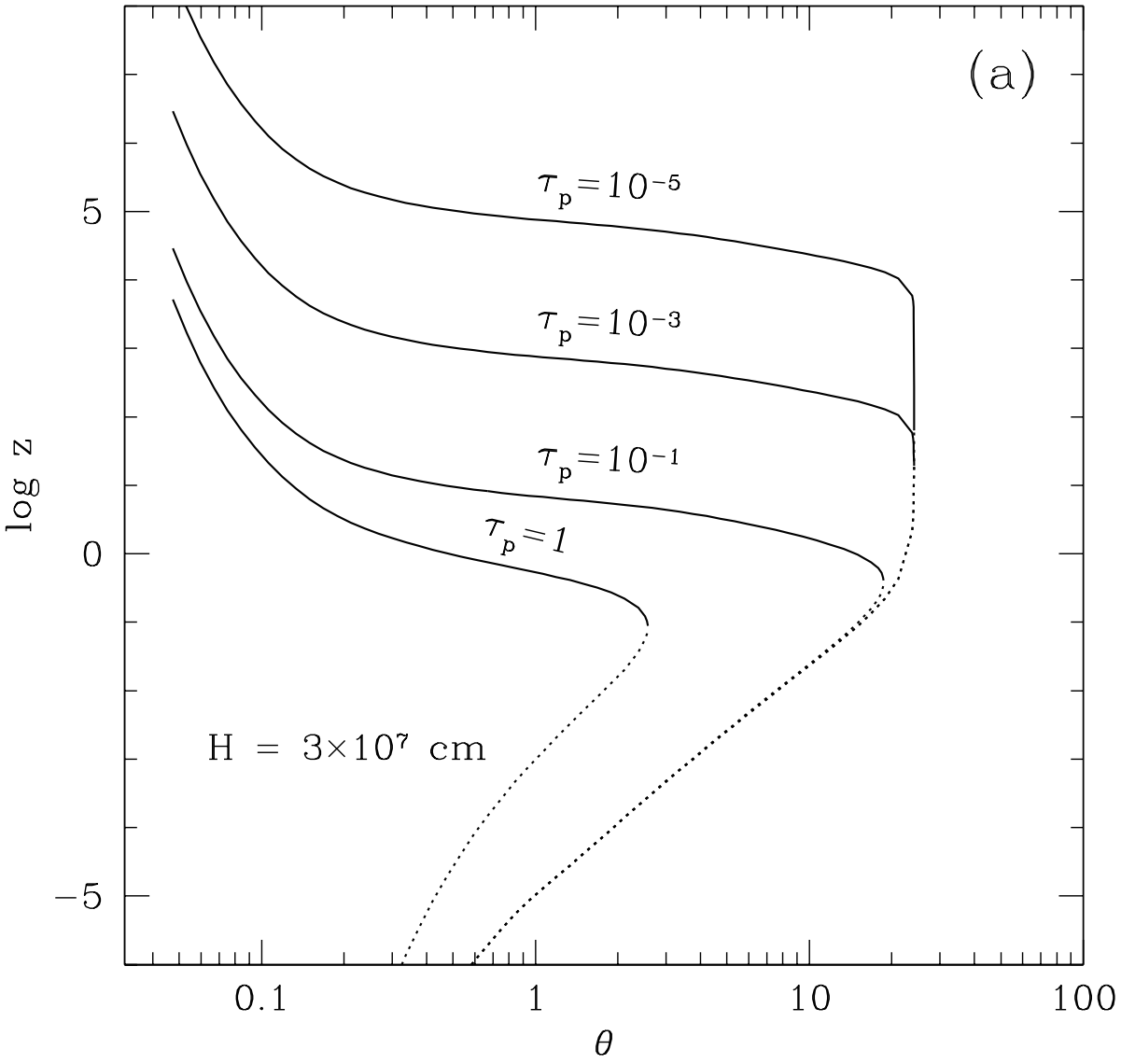

Fig. 1.— (a) The equilibrium pair fraction, $z = n_+/n_p$, in a one-temperature plasma cloud cooling via Comptonized bremsstrahlung, shown as a function of gas temperature. All four curves were computed for a cloud of size H, but with different values of the proton optical depth, as indicated on the figure. Solid lines show the high-z solution branch and dotted lines show the low-z branch.

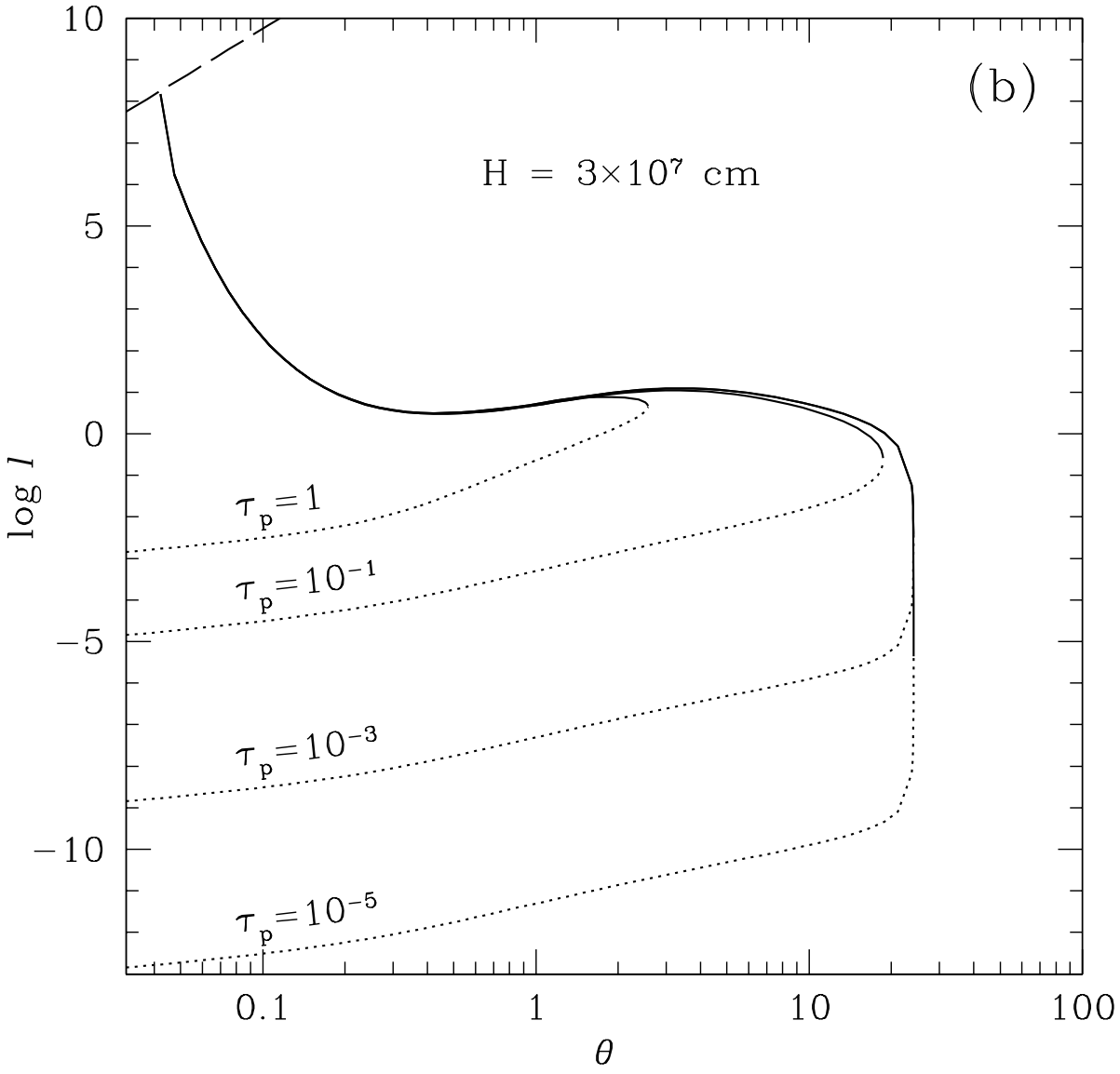

Fig. 1.— (b) Compactness as a function of plasma temperature corresponding to the equilibrium pair fraction solutions in panel (a). Solid lines correspond to the high-z branch and dotted lines to the low-z branch. The blackbody limit is indicated by a long-dashed line.

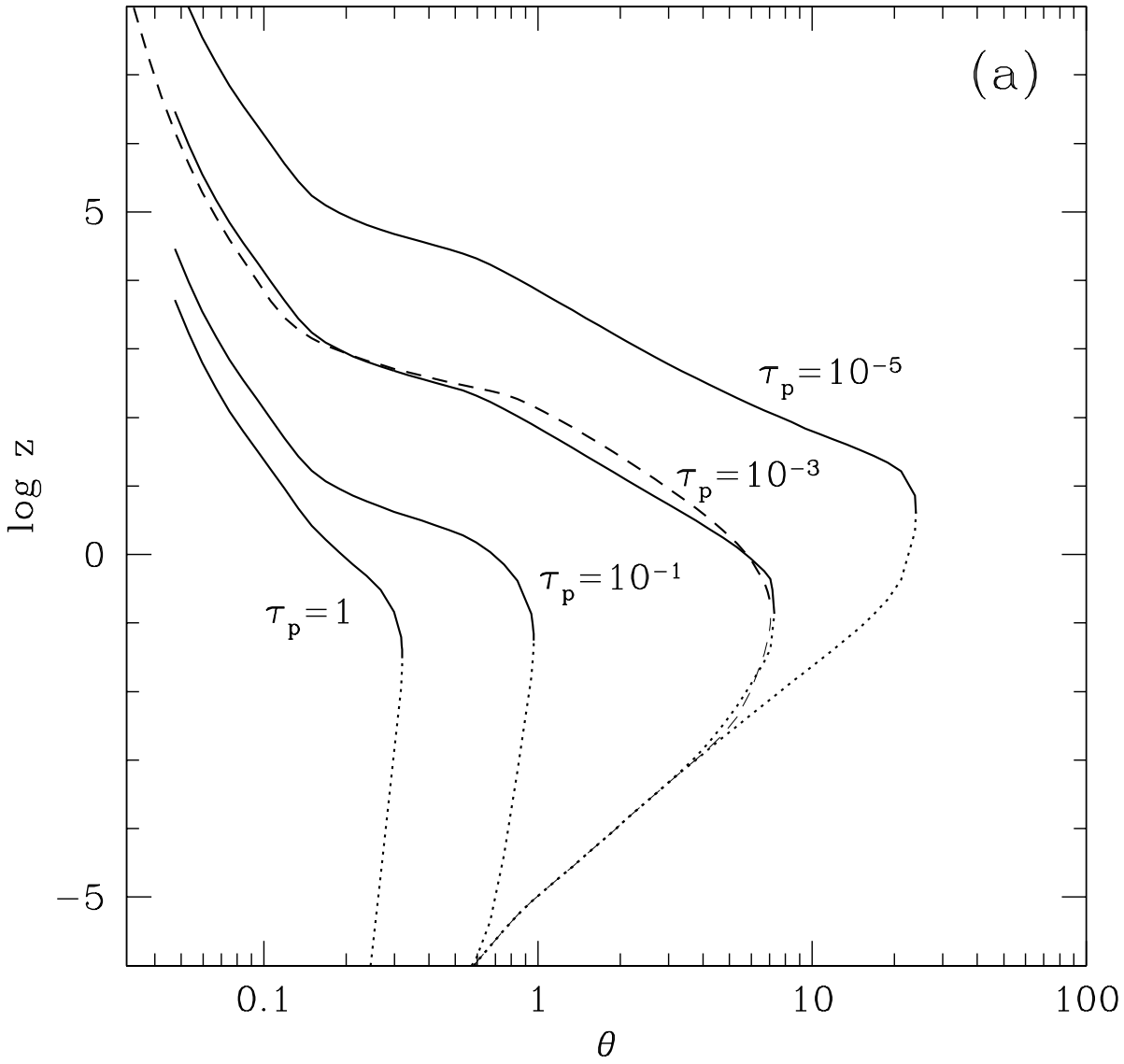

Fig. 2.— (a) The equilibrium pair fraction, $z = n_+/n_p$, in a one-temperature plasma cloud cooling via Comptonized bremsstrahlung and synchrotron, shown as a function of gas temperature. In calculating the synchrotron emissivity we assumed that the magnetic pressure is equal to the gas pressure. As in Fig. 1, solid and dotted lines show the high-z and low-z branches, respectively. These four curves were computed for a cloud of size $H = 3\times10^7$ cm, but with different values of the proton optical depth, as shown on the figure. The dashed curve shows the pair fraction computed for $\tau_p = 10^{-3}$ and $H = 3\times10^{14}$ cm.

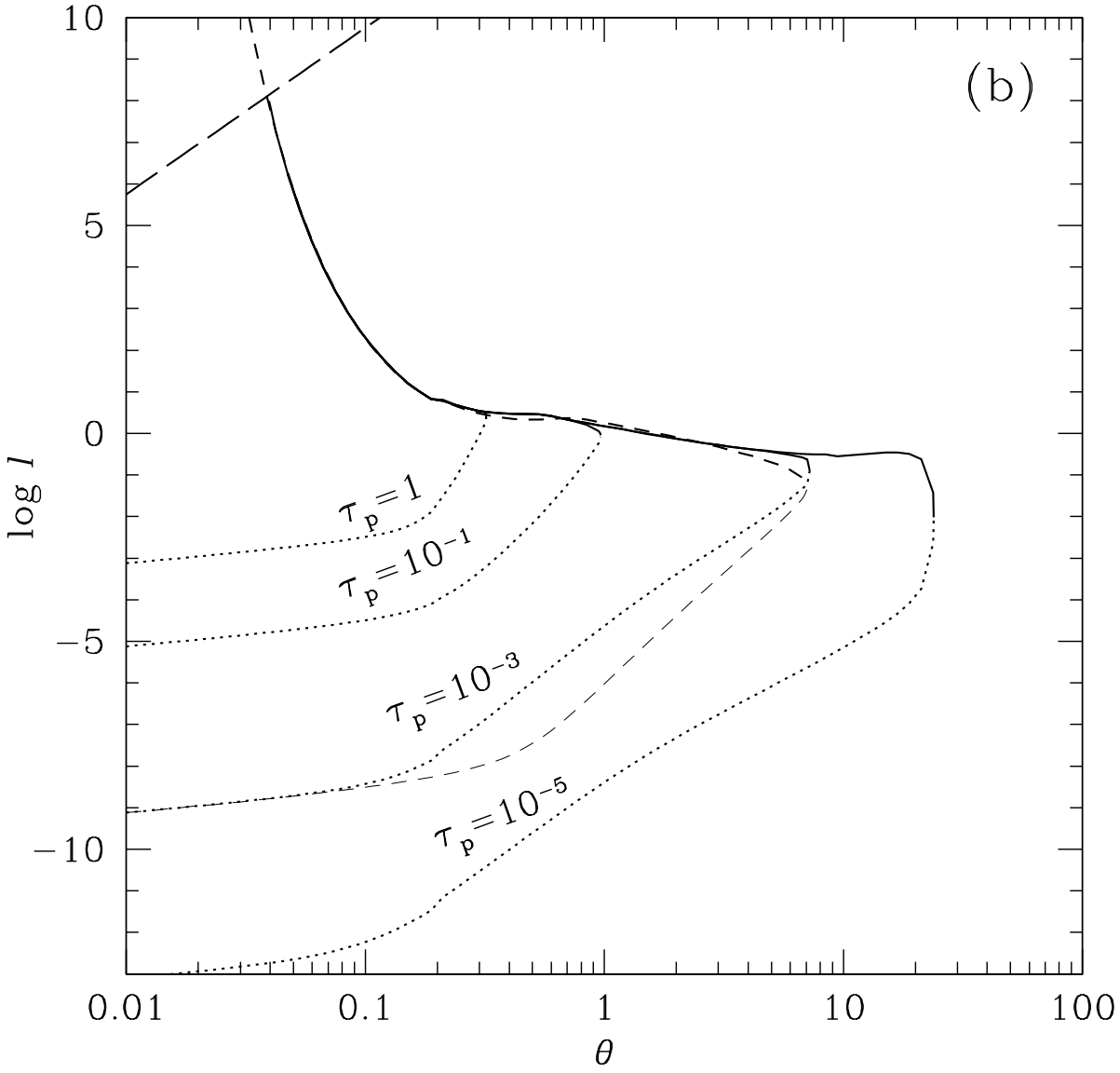

Fig. 2.— (b) Compactness as a function of plasma temperature corresponding to the equilibrium pair fraction solutions in Figure 2(a). The blackbody limit for a cloud of size $H = 3 \times 10^7$ cm is indicated by a long-dashed line.

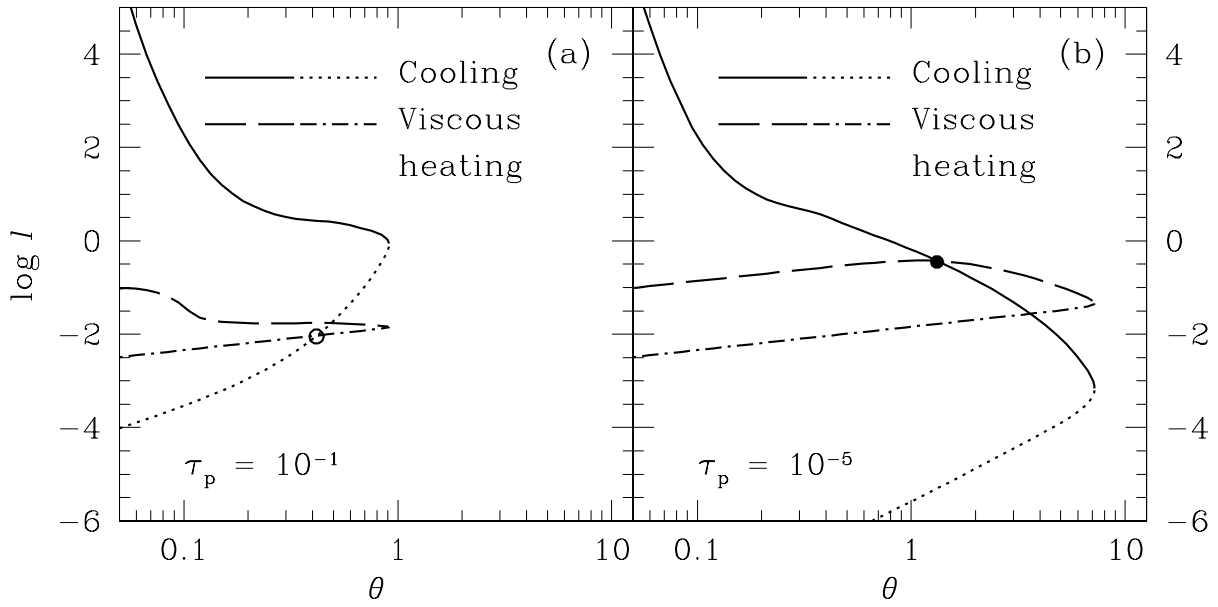

Fig. 3.— Illustrates the balance between dimentionless viscous heating, $\delta Q_G H \sigma_T/(m_e c^2)$, and cooling, ℓ, rates in a magnetized corona above a thin disk with $\dot{m}_D = 10^{-3}$, $r = 10$, $m = 10$. The values of compactness and viscous dissipation on the high-z solution branch are shown as solid and dashed lines respectively, and the corresponding quantities for the low-z solution values are shown as dotted and dot-dashed lines. (a) Shows the case of a corona with $\tau_p = 0.1$. There is a low-z equilibrium solution, marked with an open circle. This solution is practically pair-free with $z = 2 \times 10^{-5}$. Note that there is no high-z solution for this value of τ_p, since the solid and dashed curves do not intersect each other. (b) Shows high-z equilibrium solution for a corona with $\tau_p = 10^{-5}$, marked with a solid dot. The solutions corresponds to a pair fraction $z = 1.1 \times 10^3$. For this value of τ_p there is no low-z solution.

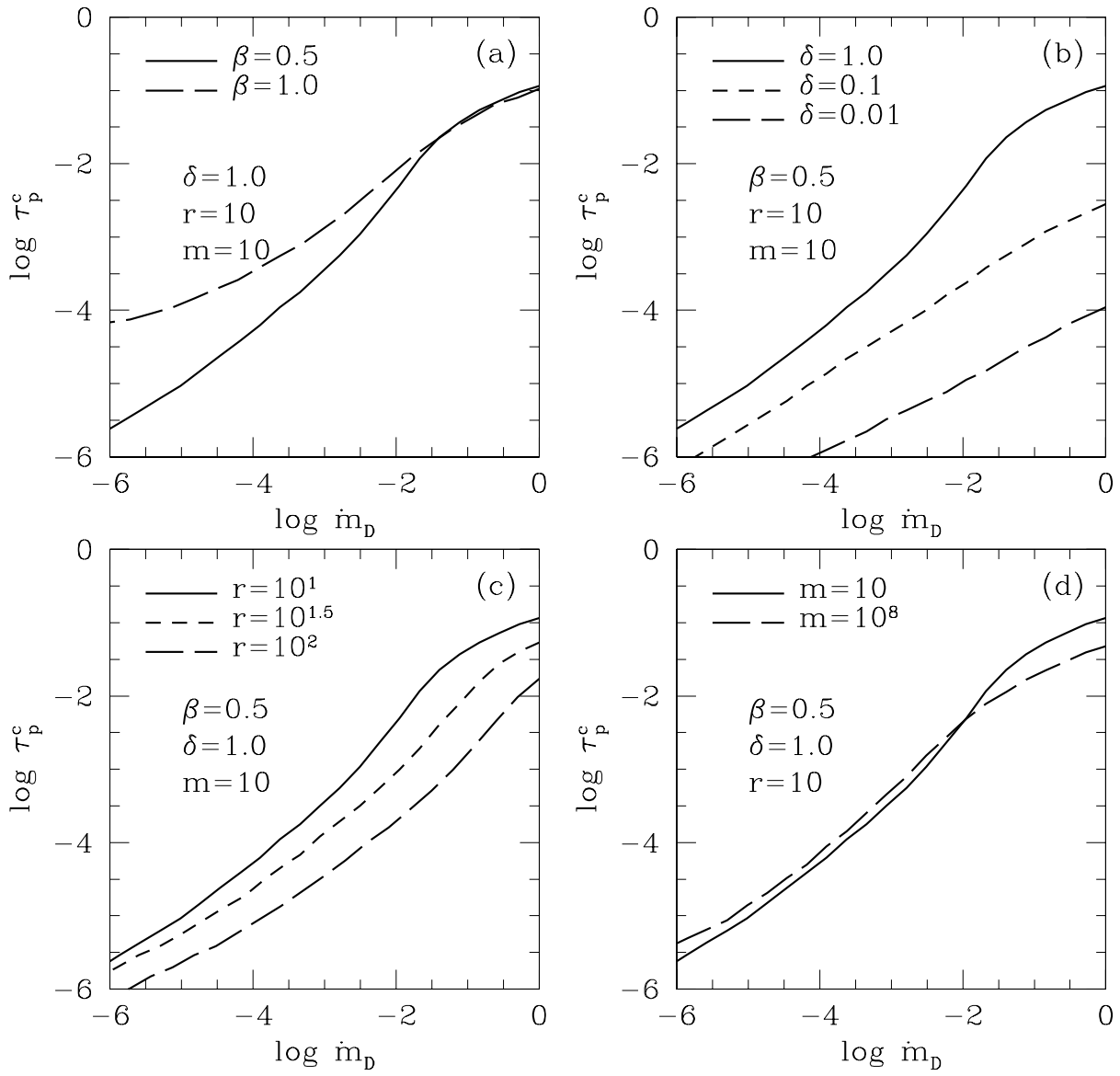

Fig. 4.— (a) Critical proton optical depth, τ_p^c, plotted as a function of $\dot{m}_D$ for a one-temperature corona. The solid line was computed for a magnetized corona with $\beta = 0.5$, assuming $\delta = 1$, $r = 10$, and $m = 10$. The dashed line shows the results for a non-magnetized corona with otherwise the same parameters. A single-temperature corona with $\tau_p < \tau_p^c$ is pair-dominated ($z > 1$), while coronae with higher proton optical depth have $z < 1$. (b) Curves of τ_p^c as a function of $\dot{m}_D$, calculated for $m = 10$, $r = 10$, and $\beta = 0.5$, plotted for different values of δ. (c) Curves of τ_p^c as a function of $\dot{m}_D$, calculated for $m = 10$, $\delta = 1$, $\beta = 0.5$, and values of r as indicated on the figure. (d) Curves of τ_p^c as a function of $\dot{m}_D$, calculated for different masses of a central black hole.

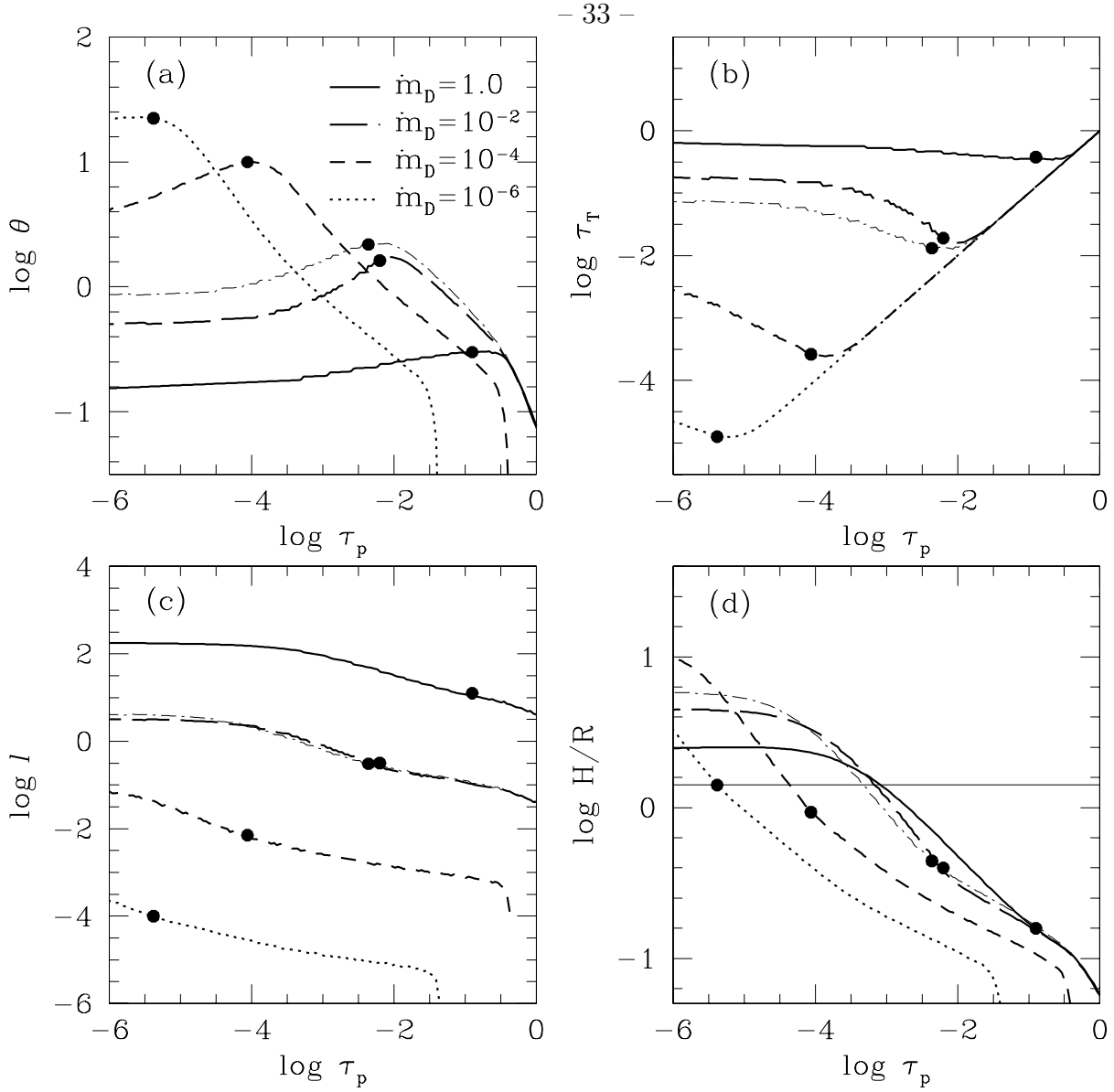

Fig. 5.— On all four panels different curves correspond to different values of the disk mass accretion rate, $\dot{m}_D$. The other parameters are fixed at $\delta = 1$, $r = 10$, $m = 10$, except for the dot-dashed curves, which are calculated with $\dot{m}_D = 10^{-2}$ and $m = 10^8$. The solution with $\tau_p = \tau_p^c$ is marked with a solid dot on each curve. (a) Equilibrium temperature, θ, in a magnetized one-temperature corona plotted as a function of τ_p. Pair-dominated solutions correspond to $\tau_p \leq \tau_p^c$. (b) Optical depth for electron scattering, $\tau_T = \tau_p(1 + 2z)$, corresponding to equilibrium corona solutions plotted as a function of τ_p for different values of $\dot{m}_D$. So long as the corona is pair-free ($\tau_p \geq \tau_p^c$), τ_T is equal to the proton optical depth. Below τ_p^c, however, pairs dominate the electron scattering opacity, and τ_T converges to a constant value. (c) Dimentionless cooling rate, ℓ, of the corona plotted as a function of τ_p for different values of $\dot{m}_D$. (d) Scale height of the corona determined from equation (2-7). The thin solid line corresponds to $H/R = 2$; only solutions below this line are dynamically stable.

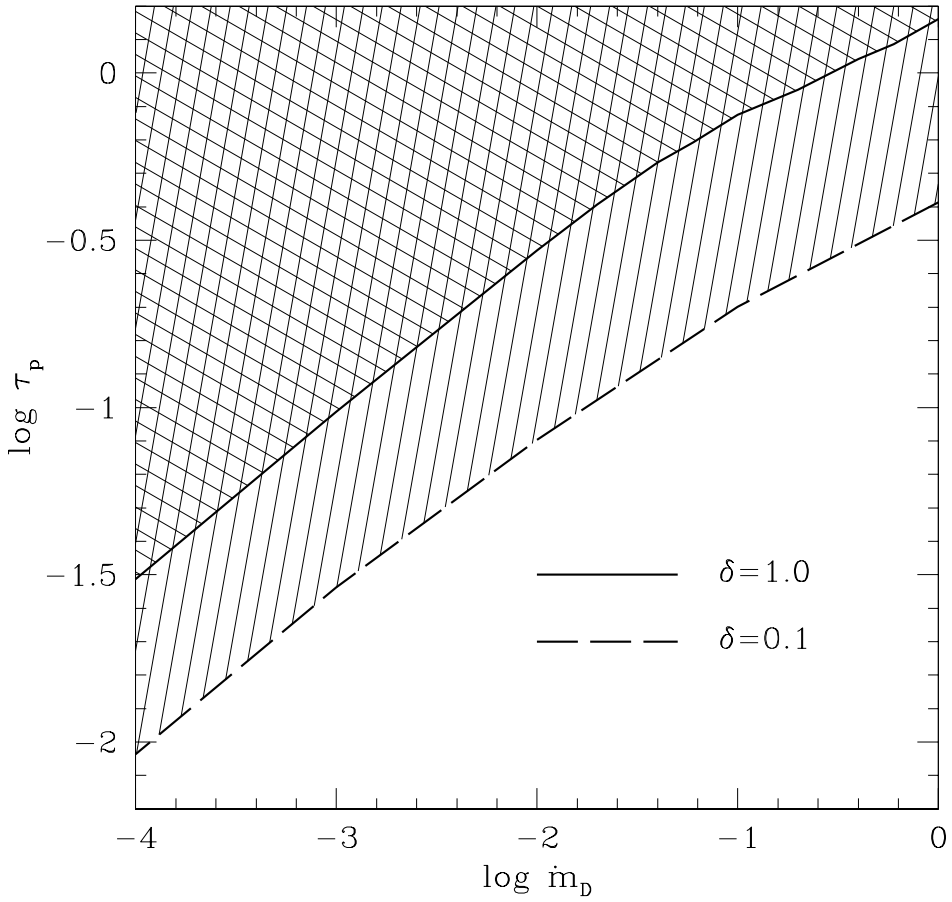

Fig. 6.— Regions of the parameter space where equilibrium solutions for a two-temperature corona are allowed, are shaded. The results are shown for $m = 10$, $r = 10$, $\beta = 0.5$ and two different values of δ, as indicated on the figure. In the region below the thick solid line, Coulomb energy transfer rate is too inefficient to allow the protons in the corona to be in thermal balance. A comparison between this panel and Fig. 4(b) clearly shows that the shaded regions lie above the τ_p^c curves for a one-temperature corona. This indicates that a two-temperature corona in thermal equilibrium always has $z \ll 1$.

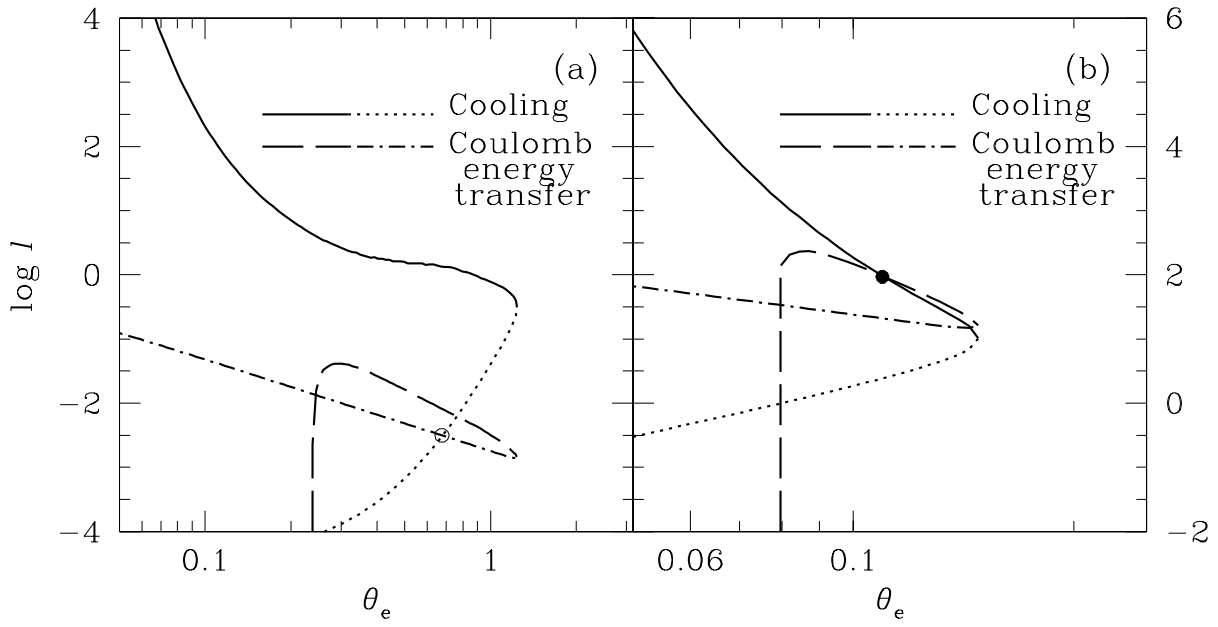

Fig. 7.— Illustrates the electron energy balance in a two-temperature accretion flow with a fixed f. Dimensionless electron cooling rate (compactness) and Coulomb energy transfer rate in pair equilibrium are plotted vs. electron temperature, θ_e. Solid and dashed curves show the high-z solution branches for cooling and heating rates respectively, while dotted and dot-dashed lines show the low-z branches. Equation (2-10) is satisfied at the intersection point. The flow parameters are fixed at $\alpha = 1.0$, $r = 10$, $m = 10$, $\beta = 0.5$; (a) $f = 0.1$, $\dot{m} = 0.01$; (b) $f = 0.03$, $\dot{m} = 0.14$. The low-$\dot{m}$ solution in (a), marked with an open circle, is pair-free, with $z = 2.5 \times 10^{-5}$; and the high $\dot{m}$ solution in (b), marked with a solid dot, has a relatively large pair fraction of $z = 1.9$.

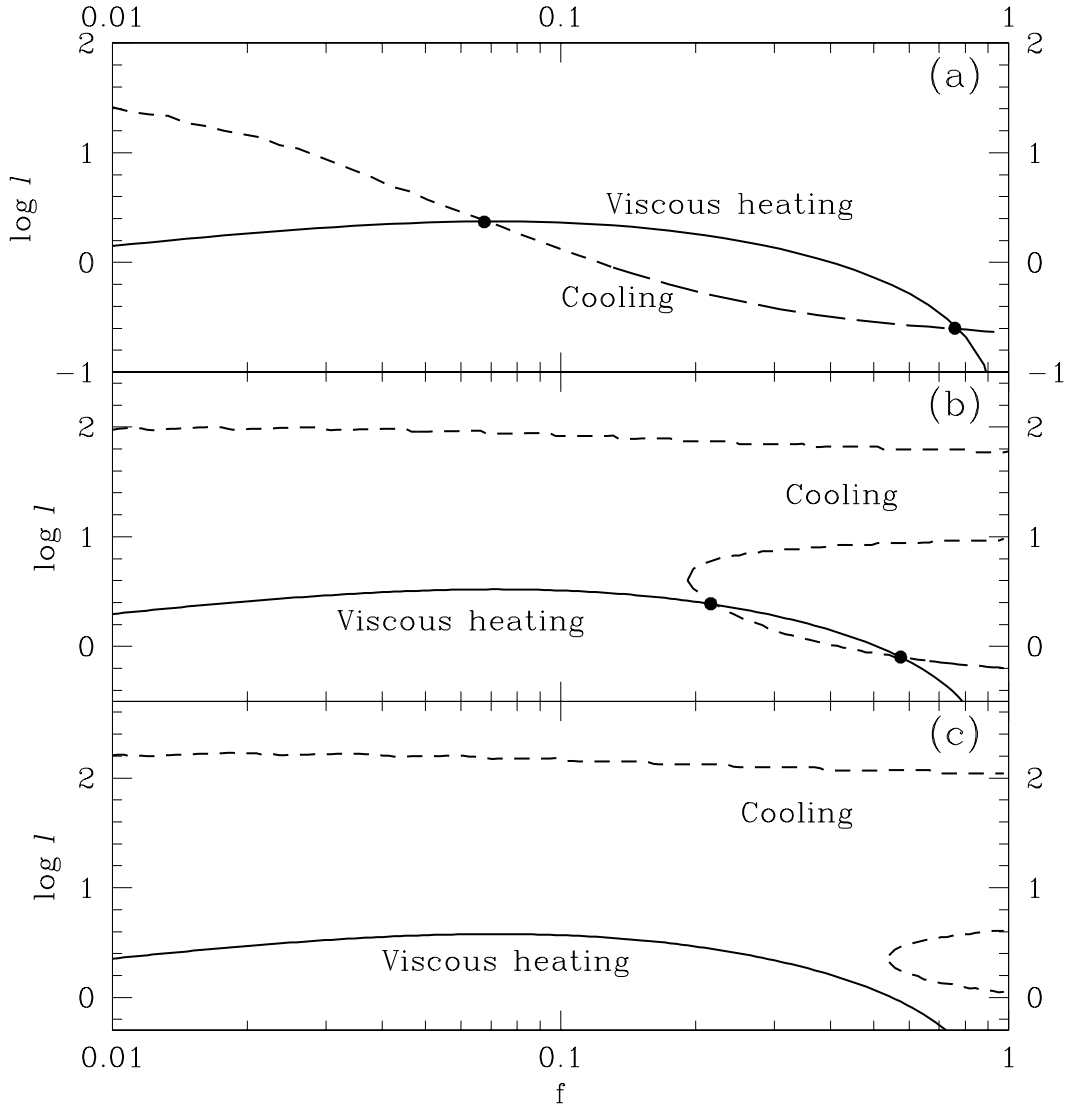

Fig. 8.— Proton energy balance in a two-temperature accretion flow for $m = 10$, $r = 10$, $\alpha = 1.0$, $\beta = 0.5$, and (a) $\dot{m} = 0.1$, (b) $\dot{m} = 0.14$, (c) $\dot{m} = 0.16$. Dimensionless heating (solid line) and cooling (dashed line) rates for the protons are plotted as functions of f. Viscous heating is given by the self-similar accretion flow solutions (Narayan & Yi 1994). Cooling through Coulomb collisions with electrons is obtained by solving the electron energy balance equation (see Fig. 7), and is equal to the local compactness of the gas. Parts of the cooling curve which correspond to the high-z branch on Fig. 7 are plotted as a short-dashed line; the long-dashed line shows the low-z compactness values. Solid dots mark the positions of thermal equilibria. Note that there are two solutions for $\dot{m} = 0.1$ and 0.14 and no solutions for $\dot{m} = 0.16$.

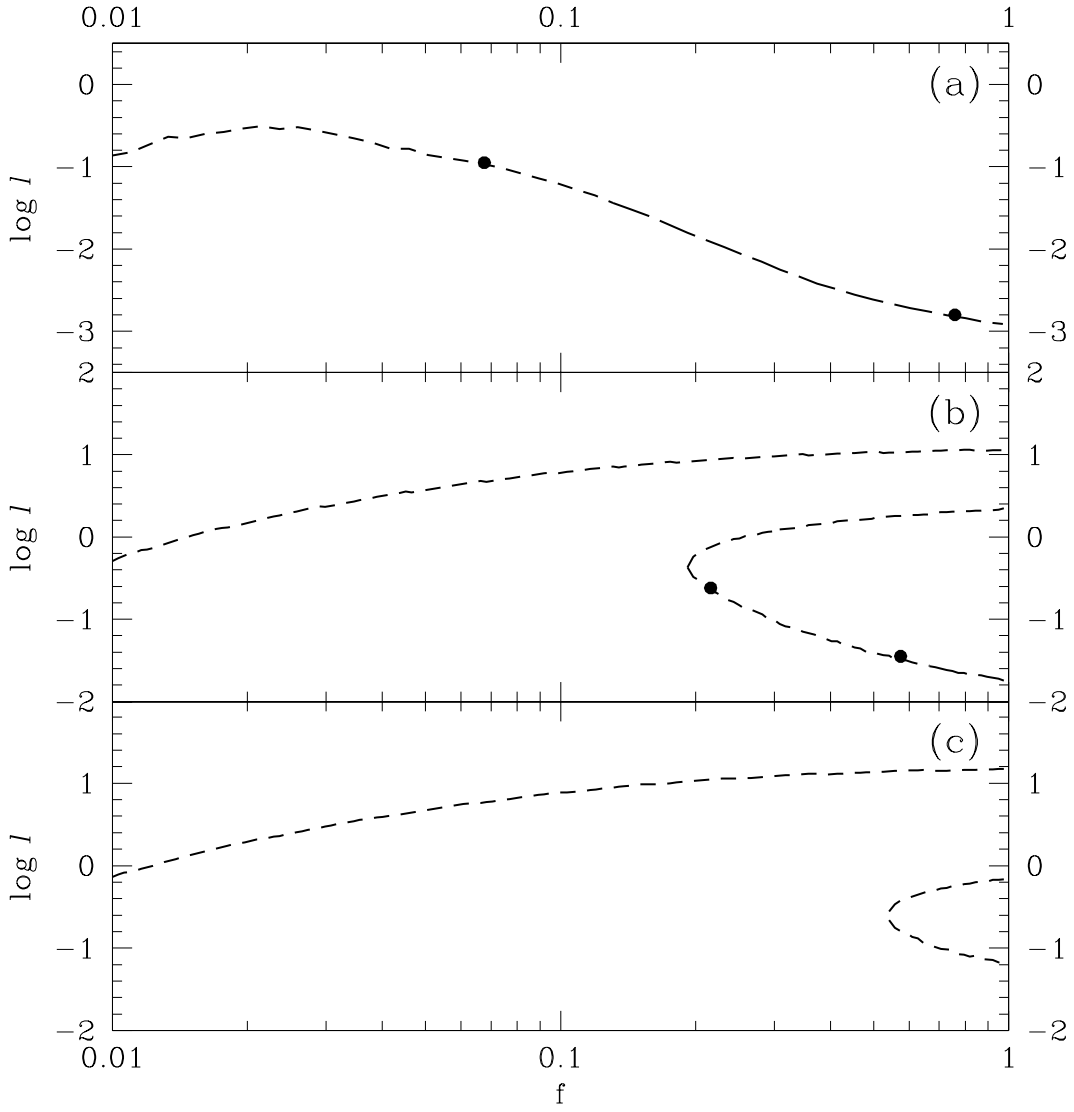

Fig. 9.— Pair fraction z corresponding to the cooling curves on Fig. 8 plotted as a function of f for the same values of the mass accretion rate: (a) $\dot{m} = 0.1$, (b) $\dot{m} = 0.14$, (c) $\dot{m} = 0.16$. Although there are cooling branches on panels (b) and (c) that have relatively high pair densities, thermal equilibria (marked by solid dots), when they exist at all, invariably have $z < 1$.

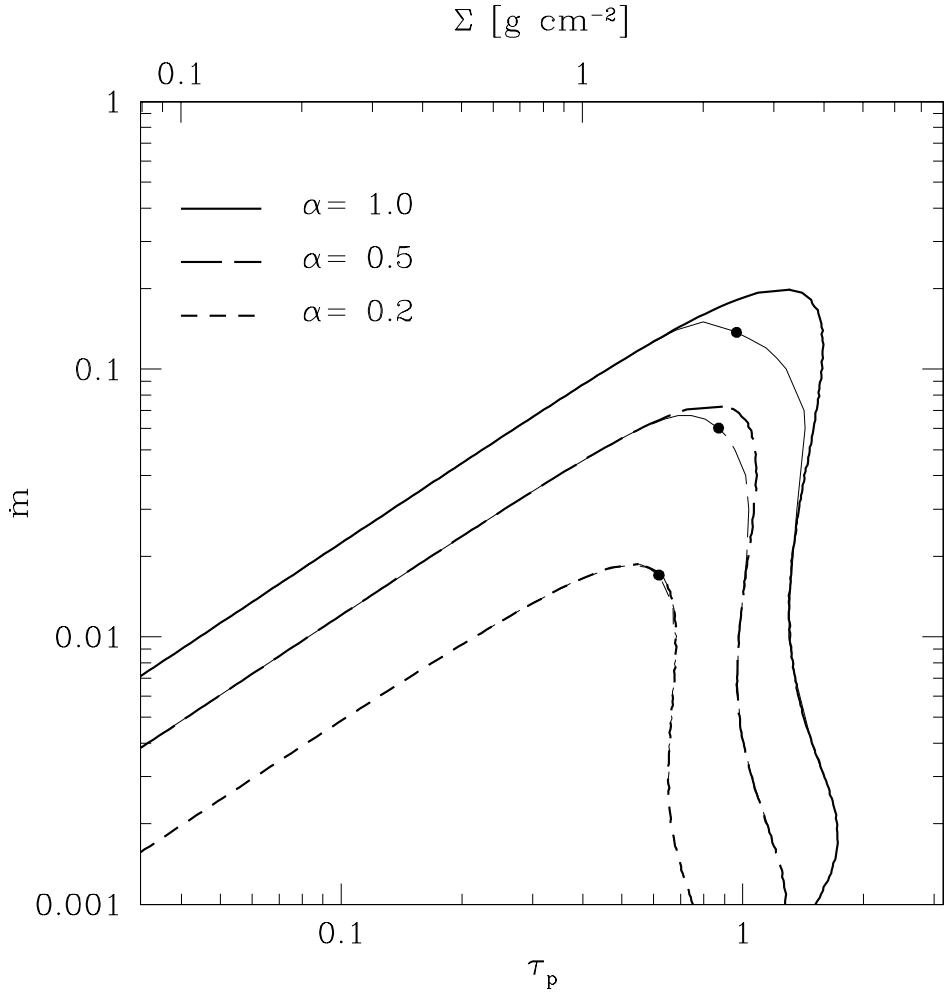

Fig. 10.— Thermal equilibria of optically thin accretion flows calculated for $m = 10$, $r = 10$, and $\beta = 0.5$.. The thick curves show the solutions computed without pairs; the thin curves correspond to the solutions with full account of pairs. The maximum pair fraction (indicated by solid dots on the figure) is $z = 0.2$ for $\alpha = 1.0$, $z = 0.06$ for $\alpha = 0.5$, and $z = 0.006$ for $\alpha = 0.2$.